IDO-16893

QUARTERLY TECHNICAL REPORT
SPERT PROJECT
January, February, March, 1963

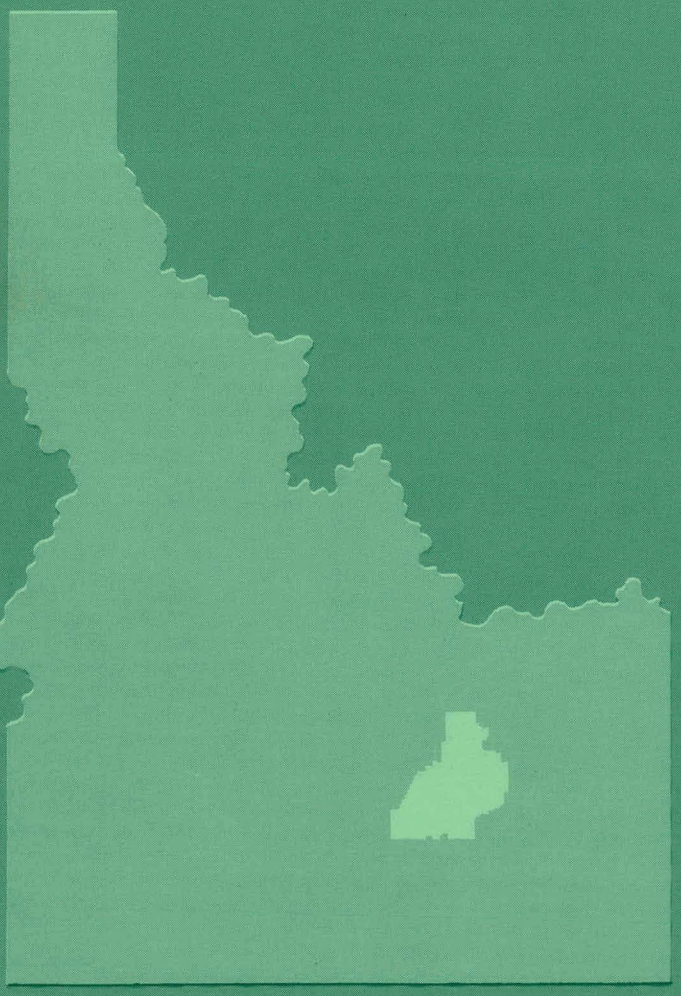

PHILLIPS PETROLEUM COMPANY

ATOMIC ENERGY DIVISION

NATIONAL REACTOR TESTING STATION
US ATOMIC ENERGY COMMISSION

DISCLAIMER

PRICE $1.25

Available from the
Office of Technical Services
U. S. Department of Commerce
Washington 25, D. C.

Printed in USA

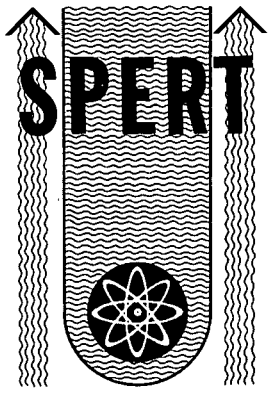

IDO-16893
AEC Research and Development Report
Reactor Technology
TID-4500 (20th Ed.)
Issued: May 20, 1963

QUARTERLY TECHNICAL REPORT
SPERT PROJECT
JANUARY, FEBRUARY, MARCH, 1963

J. R. Huffman
Assistant Manager, Technical

W. E. Nyer
Manager, Reactor Projects Branch

F. Schroeder
Manager, Spert Project
Editor

PHILLIPS
PETROLEUM
COMPANY

Atomic Energy Division
Contract AT(10-1)-205
Idaho Operations Office
U. S. ATOMIC ENERGY COMMISSION

THIS PAGE

WAS INTENTIONALLY

LEFT BLANK

QUARTERLY TECHNICAL REPORT
SPERT PROJECT
JANUARY, FEBRUARY, MARCH, 1963

SUMMARY

During the first quarter of 1963, additional data from the 3.2-msec-period destructive test were analyzed. Recovery and cleanup operations in the Spert I area were completed. Each of the 270 highly enriched, aluminum-clad fuel plates in the core was found to have experienced melting to some degree. Calculations of the maximum temperature reached by the U-Al fuel alloy during the destructive excursion ranged from about 1000 to 1300°C depending on assumptions made regarding transient heat transfer to the water. Analysis of the transient-pressure data obtained during the test and consideration of the observed deformation of core components and pressure transducer diaphragms indicate that the destructive pressure pulse reached a peak of approximately 3000 to 4000 psi. The available data on the nature of the pressure pulse and on the condition of the core fuel plates at the time of the pulse are consistent with the hypothesis that the observed destructive effects were produced by a self-propagating steam explosion resulting from the dispersal of molten fuel plates into the water throughout the core. Chemical analysis of the debris recovered from the reactor vessel indicated a content of 65 wt% Al and 6.7 wt% U, with the remainder consisting of insoluble residue, sand, glass, iron, etc. The results of X-ray diffraction analyses of the insoluble residue indicated that the recovered debris contained about 0.4 kg of α-Al_2O_3. This amount of oxide would have resulted from an aluminum-water reaction with a chemical energy release of approximately 3.5 Mw-sec. This can be compared with the observed nuclear energy release of 31 Mw-sec. The results of aluminum-water reaction experiments performed with Spert I fuel plates in the Treat reactor indicate that for the relatively low fuel temperatures achieved during the destructive test, the chemical reaction probably proceeded slowly, with a reaction time of the order of seconds, and that it occurred as a consequence of the disintegration of the fuel plates caused by the violent steam explosion. Metallographic examination of eight fuel plates from the destructive test core has been completed. There is no metallographic evidence that the fuel alloy reached the vaporization temperature. The Spert I facility is now being prepared for a second integral-core destructive test program to be conducted with the low-enrichment, uranium-oxide, rod-type core previously tested in Spert I.

A series of tests has been initiated to determine the response of the Spert IV plate-type core to step-inputs of reactivity at ambient temperature, for various initial system conditions of hydrostatic head above the core, and forced coolant circulation rate. Power excursion tests with initial reactor periods in the range from 1 sec to 8.5 msec were performed with an 18-ft hydrostatic head above the core and no forced coolant circulation. Tests with periods of 20, 12, and 8.5 msec were also performed with a 2-ft head. No significant change was observed in the peak power, power burst shape, energy release, or transient pressure behavior as a result of the head change. The fuel plate surface temperatures were slightly higher for the 18-ft head tests. Tests with periods in the range from 500 to 10 msec were performed with a forced coolant flow rate through the core of 5000 gpm (12 ft/sec) with the 18-ft hydrostatic head. For tests with periods longer than about 100 msec, the addition of forced flow tends to eliminate the initial

power peak and to increase the equilibrium power level. For shorter-period tests, the initial power peak is increased slightly when flow is added, but the effect decreases as the period is shortened. A series of damped secondary power bursts is observed in the short-period tests with flow. Fuel plate surface temperatures are reduced by the addition of flow for long-period tests, but for tests with periods shorter than about 30 msec, the available 12 ft/sec flow velocity had little effect on the temperatures.

Four-group, one-dimensional diffusion theory calculations have been performed to provide preliminary information pertinent to the selection of specifications for low-enrichment, oxide fuel rods to be used in planned future test programs in Spert III and Spert IV.

Data from a series of high-power pile-oscillator experiments previously conducted in Spert I with the P-18/19 core at a mean power level of 400 kw and a bulk-water temperature of 66°C have now been processed to extract the phase and amplitude of the overall frequency response of the system. The departure of the measured high-power transfer function from the theoretical low-power transfer function is significant only for frequencies below about 1 cps. Analysis is continuing to extract the feedback transfer function from these data for comparison with analytical expressions which describe the physical processes responsible for reactivity feedback. Computational procedures also have been developed to calculate the feedback transfer function directly from the measured step-transient power response of the reactor.

QUARTERLY TECHNICAL REPORT
SPERT PROJECT
JANUARY, FEBRUARY, MARCH, 1963

CONTENTS

FIGURES

TABLES

I. SPERT I

1. INTRODUCTION

An integral-core destructive test was performed in the Spert I facility in November 1962, on a highly enriched, plate-type, water-moderated core. Results of the preliminary analysis of the data from this test were presented in the previous quarterly report. During the first quarter of 1963, detailed examination and analysis of the data continued while recovery and cleanup operations in the reactor area were completed. This section of the report presents (a) a brief review of the principal results reported previously, (b) a description of the recovery and cleanup operations performed in the Spert I reactor area, (c) a description of the extent of fuel plate melting observed in the destructive test and in the two limited-melting tests performed prior to the destructive test, (d) additional data on the maximum temperatures obtained in the reactor fuel, (e) data pertaining to the magnitude, nature, and source of the explosive pressure pulse, (f) the results of the analysis of the metallic debris recovered from the reactor vessel for metal-water reaction products, (g) a brief description of the results of metallographic examinations of fuel plates from the destructive test, and (h) a brief description of the preparations presently underway for future testing in the Spert I facility.

2. BRIEF REVIEW OF PRINCIPAL RESULTS OF THE DESTRUCTIVE TEST

The power excursion of the Spert I destructive test was self-limiting in character, with burst characteristics which were essentially predictable from longer-period non-destructive test data. As reported previously [1], data obtained during the power excursion indicate a reactor period of 3.2 msec, a peak power of 2.3 Gw, a nuclear energy release to the time of peak power of 14 Mw-sec, a total burst energy of 31 Mw-sec, and an initial pressure pulse (associated with self-shutdown) of about 35 psig. In addition to the transient pressure pulse observed during the power excursion, a large amplitude pressure burst occurred shortly after the nuclear excursion which caused destruction of the core and extensive damage to the core support structure, in-pile instrumentation, and the control system. Aside from some minor damage to overhead roof support beams, almost all mechanical damage resulting from the tests occurred within the reactor vessel. The vessel itself, which was earth-backed, had failed along one weld and was found to be bulged as much as 3 in. on the diameter at a point about 20 in. from the bottom of the tank. The fuel assemblies near the center of the core were blown apart, whereas outer assemblies were severely bent and twisted. Some of the fuel assembly lower end boxes were found to have been sheared off. The core grid assembly was fractured at the corners. Buckling of the control rods and control rod drive extensions occurred when the lower bridge, which provides bearing support for the control rods, was propelled upward by the expulsion of water from the tank.

3. RECOVERY AND CLEANUP OPERATIONS

Recovery and cleanup operations in the Spert I reactor vessel and surrounding area were initiated soon after the destructive test in order to document in detail the condition of the core following the test. For the first few days following the test, operations consisted primarily of the acquisition of information pertaining to the reactor condition and the recovery of radiation-sensitive items from the reactor area. These efforts included removal of motion picture films and various activation samples, and a general documentation of the reactor condition by both motion pictures and still photography. Some of these photographs of the core were presented in the previous quarterly report [1]. Upon completion of these initial operations, it was necessary to recover those test components which had been ejected from the reactor tank and to make the necessary preparations for the more extensive core disassembly operations to follow. The items which had been expelled from the core were noted as to location and identity, photographed, and removed to storage. After removal of certain items of equipment from the reactor building, several areas of the building were decontaminated to prevent the spread of the low-level contamination which was present.

Systematic recovery of all items from the reactor vessel was then initiated. The position and identity of each item was recorded as it was removed to storage. All recovered fuel-bearing materials also were weighed. During these operations the radiation level directly over the reactor tank was approximately 100 mr/hr. This relatively low direct radiation level and the quite low contamination levels which were present permitted the operation to proceed relatively rapidly with no unusual radiological problems.

Fifteen of the 25 fuel assemblies in the core were found to be partially intact. Two of these assemblies were removed and transferred to the TAN hot shop where they were cut open and photographed, using remote handling tools. The remaining 13 fuel assemblies were opened at Spert. The procedure used was to place a fuel assembly in a tank of water and to grind two of the corners from the fuel assembly can permitting the can to be easily opened. A stationary electric motor was used to drive the grinding wheel through a 4-ft flexible shaft. In this operation, the water served not only as a radiation shield but also to retain radioactive dust and chips resulting from the grinding operation. On completion of the grinding operation, the assembly was dried, using heat lamps, and then photographed. The fuel plates were then separated from the aluminum can and weighed, and the fuel and assembly parts removed to storage in appropriate areas. At frequent intervals during the recovery operation photographs were taken of the status of the reactor tank in order to document, in detail, the positions of various components. Samples of the metallic residue in the reactor vessel were taken periodically, in order to obtain representative samples from all parts of the reactor vessel for subsequent analysis. Upon completion of the recovery operation, radiation levels in the reactor vessel were found to be near background and the facility was in such a condition as to allow restoration and repairs to proceed for the next test program (see section 9).

4. FUEL MELTDOWN DATA

Melting of fuel plates occurred for three of the power excursion tests conducted in the destructive test series.

For the 5-msec-period excursion test, melting was confined to a region about 6 in. high in the center of the core and involved less than 0.5% of the total fuel area of the core. Seven plates were melted during the test. Photographs of damaged fuel plates from this test were presented in a previous quarterly report [2]. Figure 1 is a cross section drawing of the Spert I core showing the radial distribution of the melted regions for this test. Figure 2 shows the vertical distribution of the melted regions of the plates.

For the 4.6-msec-period test, partial melting was obtained in 52 of the 270 fuel plates of the core, and involved about 2% of the total fuel plate surface area of the core. Photographs of melted fuel plates from this test also have been presented previously [3]. Figure 3 is a cross section drawing of the Spert I core showing the radial distribution of the melted regions for this test. (The recorded orientation of the fuel assembly in core position D-6 was rotated 180° from that shown in the figure. Experimental information on neutron flux distribution, however, is not consistent with the melting pattern unless the orientation of the assembly was as shown in the figure.) Figure 4 shows the vertical melt pattern for each of the assemblies in which melting occurred.

For the 3.2-msec-period destructive test, all of the 270 fuel plates in the core experienced melting to some degree. Figure 5 is a photograph of the top

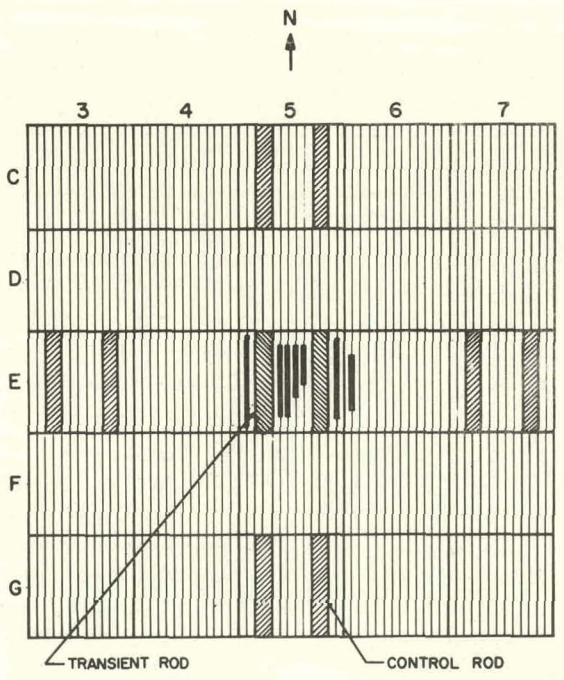

Fig. 1 Radial distribution of melting for 5-msec-period test. (Heavy black lines indicate melted region.)

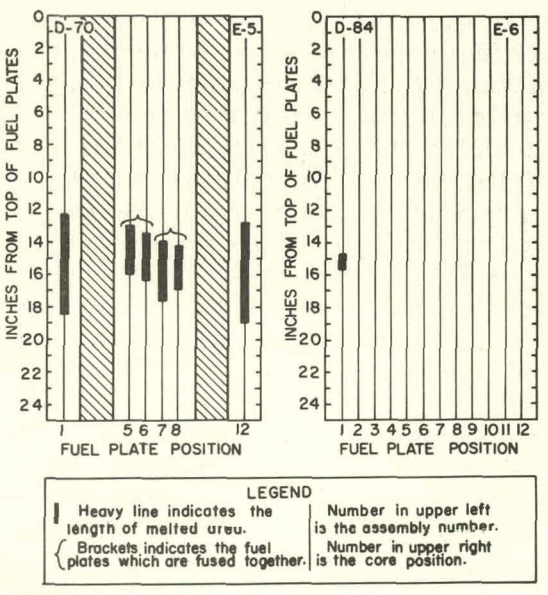

Fig. 2 Vertical distribution of melting for 5-msec-period test.

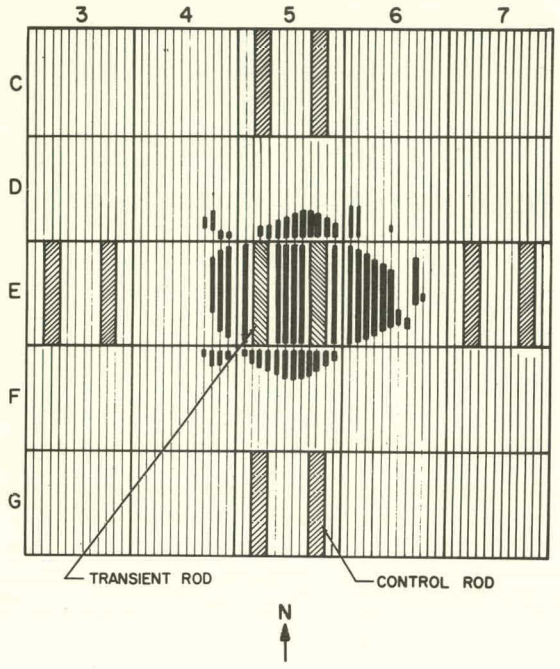

Fig. 3 Radial distribution of melting for 4.6-msec-period test. (Heavy black lines indicate melted region.)

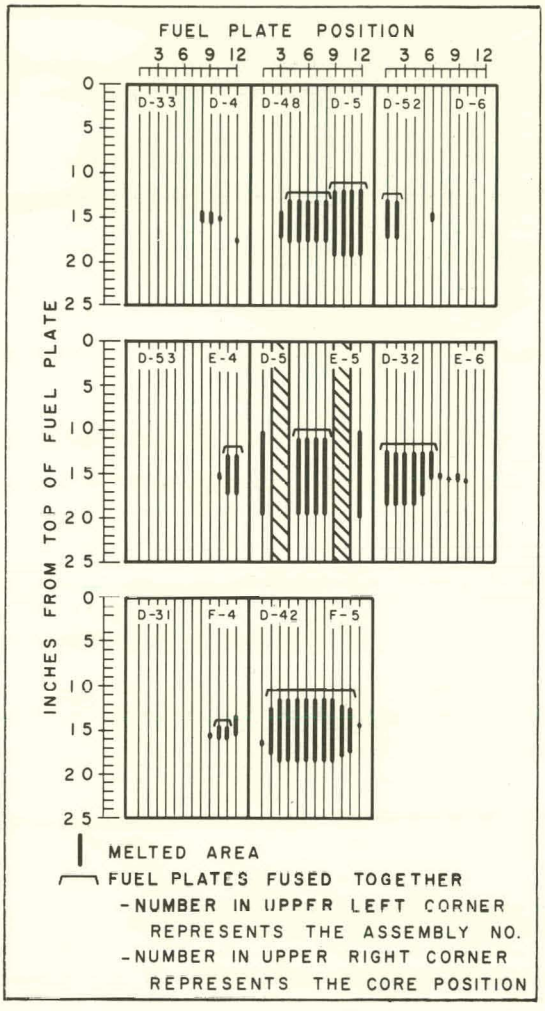

Fig. 4 Vertical distribution of melting for 4.6-msec-period test.

portions of typical fuel plates recovered from the reactor vessel. The unfueled edges of the plates can be seen to be still attached to the upper portions of the plates. The vertical pattern of fuel plate meltdown for the destructive test is shown in Figure 6 for the recovered portions of the fuel plates which could be identified. The remaining pieces of fuel plates which were recovered, but which could not be identified as to position in the core, represent about 19 wt% of the recovered plates. In the figure, the vertical melt pattern is shown for each fuel plate of each assembly with the assemblies arranged in the positions appropriate to a horizontal cross section drawing of the core. The melt pattern was symmetrical about the central fuel assembly, which showed the largest amount of melting (approximately 78 wt%). Figure 7 is a photograph of the assembly from core position D-7 (see Figure 3 for location nomenclature). This assembly was recovered relatively intact and was cut open for disassembly before the photograph was taken. It can be seen that much of the melted region of the plates is missing but that most of the unmelted upper and lower ends of the plates are still connected by the unfueled edges. Figure 8 is a photograph of several fuel plates for which much of the melted regions were still held together. The fuel plates of two of the corner assemblies of the core remained intact even though the central portion of the plates was melted. Figure 9 is a photograph of fuel plates from one of these two corner assemblies. During handling of these plates the center portions were observed to crumble and flake easily.

More complete data on the nature of the melting observed in these three tests is contained in a report presently in preparation [4].

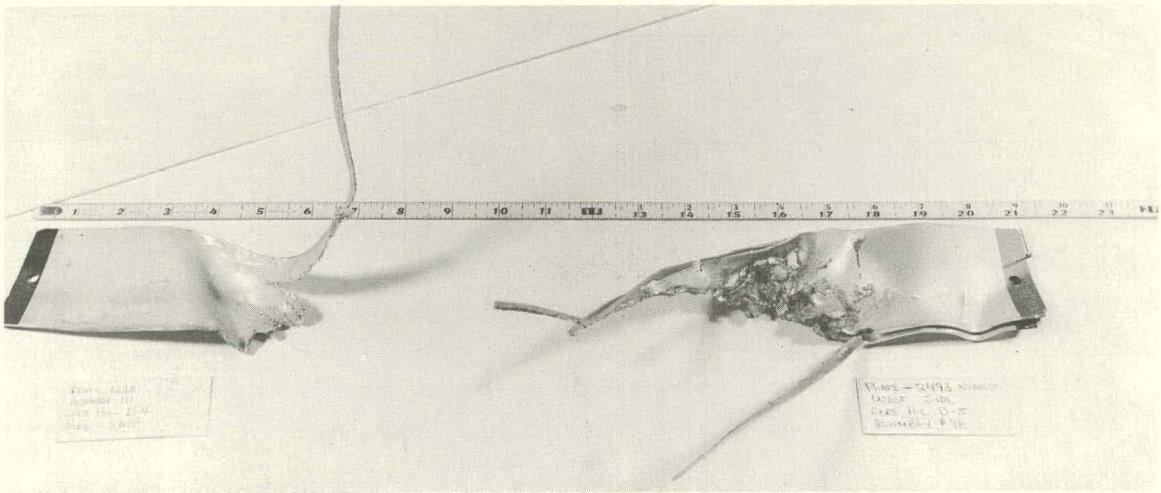

Fig. 5 Photograph of the top portions of typical fuel plates recovered from reactor vessel.

5. MAXIMUM TEMPERATURE DATA

As reported previously [1], an attempt was made to obtain a measure of the maximum fuel temperatures during the destructive test by means of a special fuel-bearing capsule containing a small quantity of fuel alloy (from a conventional plate) in contact with high melting point thermocouples. The capsule was designed to maintain good contact between the fuel alloy and the thermocouples as the fuel melted. Data obtained from this fuel capsule during the destructive test indicated a maximum capsule fuel temperature of approximately 1230°C. Upon disassembly of the capsule it was found that the fuel alloy had melted but that the stainless steel in the capsule had not, indicating a temperature of less than 1400°C. A calculation of the average fuel plate temperature at the core hot spot at the time of peak temperature has been made on the basis of no heat loss from the fuel plate during the excursion. Using the known nuclear energy release for the excursion, this calculation yields a maximum fuel temperature of approximately 1250°C. Detailed machine calculations were also made of the transient temperature profile within the fuel plate, making reasonable assumptions regarding the extent of conductive and boiling heat transfer from the

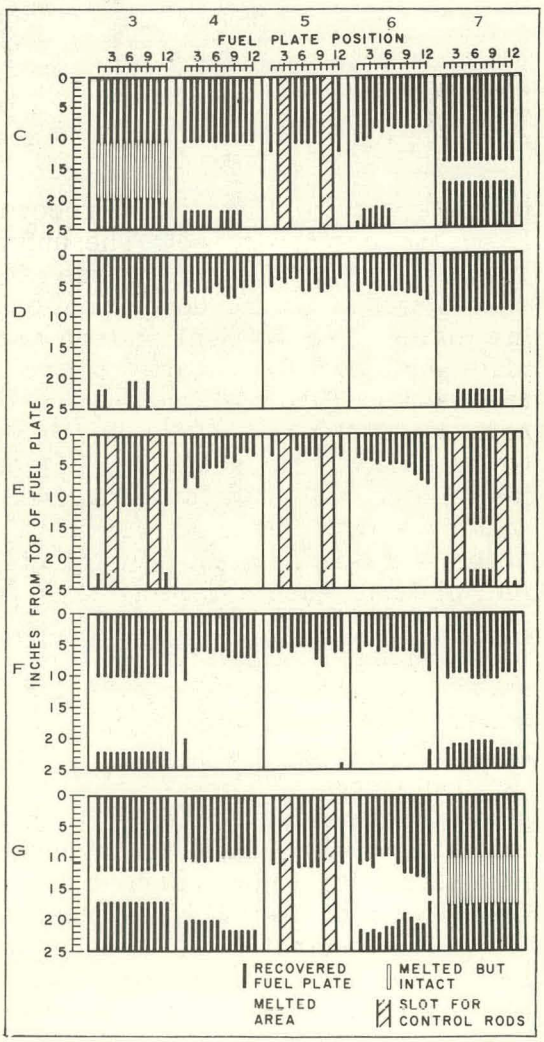

Fig. 6 Vertical distribution of melting for 3.2-msec-period destructive test.

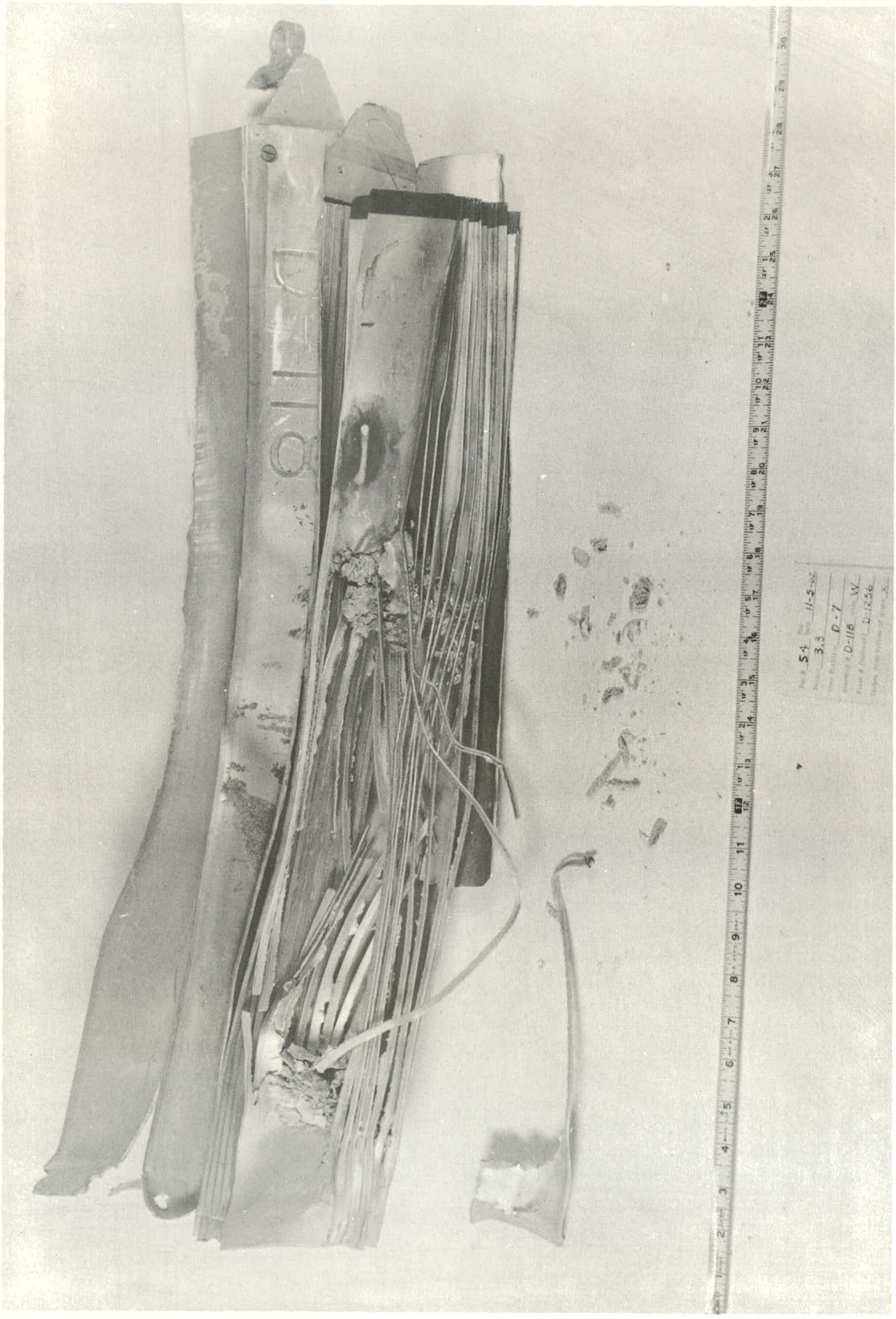

Fig. 7 Photograph of fuel assembly from core position D-7 after exterior can has been cut open for examination.

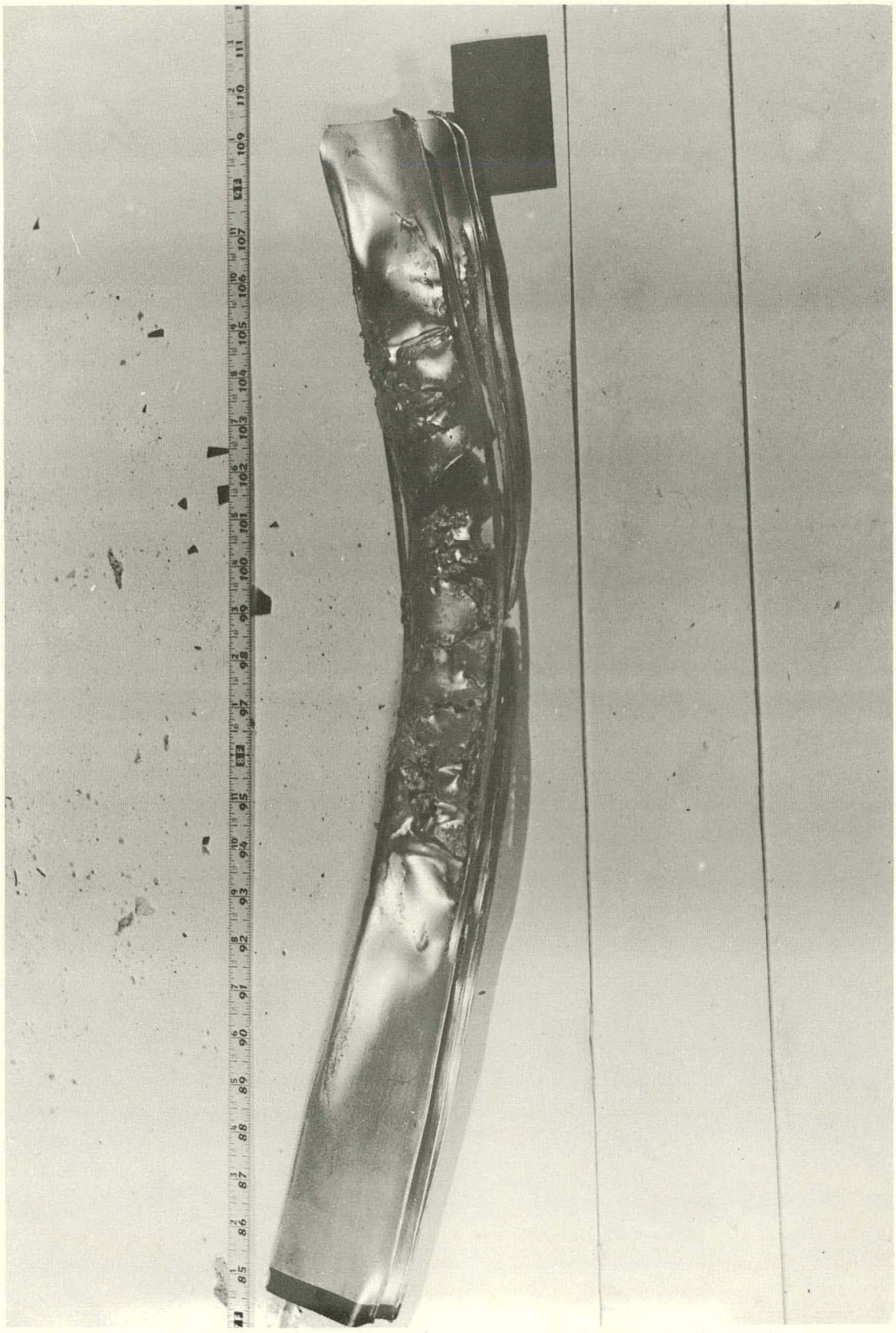

Fig. 8 Photograph of fuel plates from fuel assembly in core position G-6.

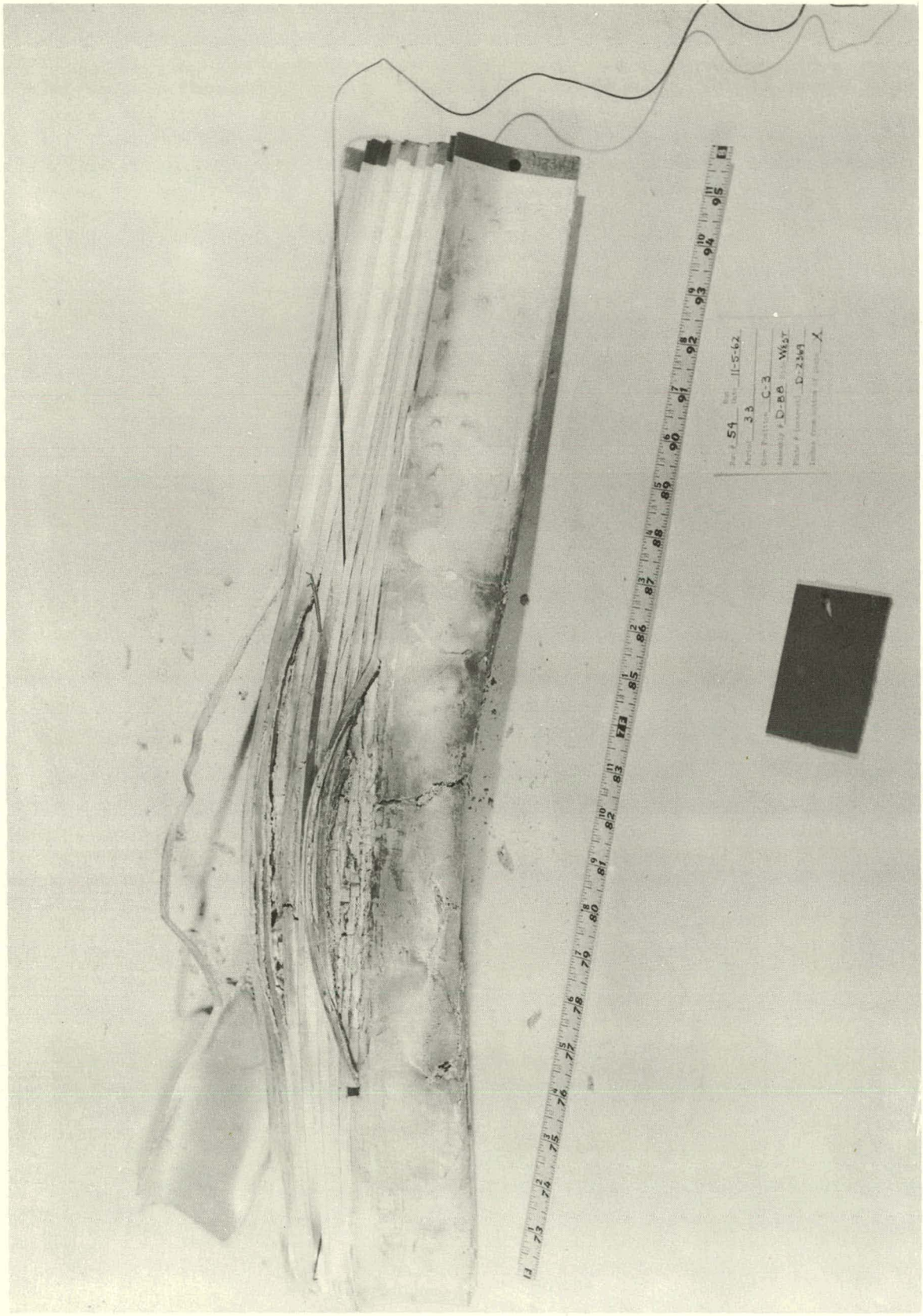

Fig. 9 Photograph of fuel plates from fuel assembly in core position C-3.

plate during the destructive excursion. The results of these calculations, while quite approximate because of the assumptions made, do indicate that the peak fuel plate temperatures were probably less than those calculated for the adiabatic case, and possibly as low as 1000°C. The value of 1230°C obtained from the fuel-bearing capsule data is probably intermediate between the actual and the adiabatic case, since the fuel within the capsule was thermally insulated to a greater extent by the stainless steel of the capsule than was the fuel within the aluminum cladding of the fuel plates.

6. PRESSURE DATA

As reported previously, approximately 15 msec after the time of the power peak a pressure surge occurred which was of the order of several thousand psi and had a very short rise time. During the present quarter, detailed examination has been conducted of all pressure data obtained during the test.

A number of pressure transducers were employed during the test to cover a range of possible pressure from a few psi to over 10,000 psi. The resonant frequencies of most of these transducers were in the range from 15 to 20 kc. The construction of these unbonded, strain-gauge-type transducers, however, permits internal damage to occur when the transducer is subjected to pressure pulses with frequency components approaching that of the resonant frequency of the transducer. Most of the pressure transducers in use for the test were internally damaged by the final destructive pressure pulse, independently of their range and without apparent external damage. Damage apparently occurred almost immediately for several of the transducers, as evidenced by signal records which became discontinuous very shortly after the initiation of the pressure pulse.

Because of the erratic nature of nearly all of the pressure transducer signals immediately after the initiation of the destructive pressure pulse, quantitative reduction of the pressure data from the recording oscillograph traces was extremely difficult. With the exception of a single 100,000-psi-range transducer, which yielded a signal too small to be accurately measured, only one other transducer signal could be identified with reasonable certainty throughout the region of interest. From the trace of this transducer it was possible to discern several high-amplitude pressure oscillations with a maximum peak pressure of about 2800 psi. The peak of this trace occurred approximately 300 μsec after initiation of the pressure pulse.

During recovery operations it was possible to obtain and analyze various pieces of damaged hardware for additional indications of the maximum pressures obtained. Calculations were made to determine the minimum static pressures required to cause the observed deformations of various components. The results of the calculation for a collapsed steel instrument tube located inside the core indicated that the dynamic pressure pulse inside the core produced damage to the tube equivalent to that which would have been produced by a static pressure of at least 3600 psi.

Since the pressure transducers used in the reactor during the test were of the diaphragm type, they could be utilized not only as normal transducers but also as peak reading deformation gauges whenever over-ranging was sufficient

to cause permanent deformation of the diaphragm. A laboratory study of these transducers at Spert has indicated that diaphragm deformations can be calibrated for over-range static pressure and that this static calibration is maintained, usually to within 10%, when diaphragm deformation is caused by pressure pulses designed to simulate the destructive pulse (with rise times as short as 100 μsec). From these calibrations and from the measured permanent deformations observed on six different transducers, it has been concluded that the pressure at a point approximately 9 in. from the edge of the reactor core reached a peak of approximately 4000 psi. Similar data from transducers 16 in. from the edge of the core indicated a maximum pressure of approximately 2200 psi. A pressure of about 3200 psi was deduced from the transducer positioned near the concrete floor of the reactor vessel, approximately 4 ft below the core.

Considerations of the nuclear energy source obtained during the test, and of the time required for redistribution of this energy within the fuel plates, indicate that, at the time of the onset of the explosive pressure pulse, the core consisted of fuel plates which were relatively strong at the top and bottom extremities, but molten over the central region, the extent of the molten portion of the fuel plate depending on the location of the plate in the core. Under these conditions the molten regions of the core were susceptible to both plastic flow and to rapid dispersion into the core water, permitting the rapid generation of steam and consequent large pressure such as that observed. The initial dispersion of the fuel into the water could have resulted from a number of possible mechaisms, eg, surface tension, mechanical vibration, small pressure surges resulting from local boiling, the action of gravity, or a local steam explosion resulting from entrapment of water within a molten metal environment. This latter mechaism is not as obvious as the others, but it can be seen to be reasonable by consideration of the nature of the fuel damage observed in the non-destructive tests performed. The fuel plate thermal distortions observed could easily cause blockage of moderator channels. In cases where the fuel plates reached melting temperatures (particularly in the 4.6-msec-period test) extensive channel blockage and adhesion between slightly molten adjacent plates was found to occur. In the destructive test such occlusion of water channels could have accompanied the melting of the fuel plates in the central core region with the consequent entrapping of small quantities of water in a molten environment. This would provide a means for a local steam explosion arising from vaporization and superheating of water in these blocked channels. Such steam explosions with molten aluminum in water have been previously observed [5].

The available information on the nature of the pressure pulse and on the condition of the core fuel plates at the time of the pulse leads to the hypothesis that the observed destructive effects were produced by a self-propagating steam explosion resulting from the dispersal of molten fuel plates into the water throughout the core.

7. ANALYSIS OF DEBRIS AND DATA ON METAL-WATER REACTION

Approximately 20 kg of debris, ranging in size from a few centimeters to less than 3 mils in diameter, was removed from the reactor vessel during recovery operations. Most of this debris consisted of spongy metallic particles with a dull-gray finish similar to the type of residue material obtained in various

studies of the aluminum-water reaction [6]. In addition, the debris contained sand (blown by the wind into the open tank), pieces of glass, and small metallic fragments of core support structure and instrumentation. Chemical analysis of several representative samples of the debris, totaling about 1.4 kg, indicated a content of 65 wt% aluminum and 6.7 wt% uranium, with the remainder consisting of insoluble residue, sand, glass, iron, etc. The results of X-ray diffraction analyses of the insoluble residue indicated that the total debris included approximately 0.4 kg of α-Al_2O_3, which is a solid reaction product of the exothermic aluminum-water reaction. This corresponds to an oxidation of about 0.2 kg of aluminum, or approximately 0.4% of the aluminum in the core. About 3.5 Mw-sec of chemical energy (or approximately 10% of the nuclear energy developed in the power excursion) would have been released in a metal-water reaction of this extent.

While this amount of chemical energy, if transformed into mechanical energy, could account for the observed destructive consequences of the test, the results of several investigations of the metal-water reaction indicate that the very high burning rates which would be required to produce the short-rise-time pressure pulse observed in the Spert I (and Borax I) destructive tests could probably be attained only if the aluminum were at a temperature quite near the vaporization point, and finely dispersed into particle sizes of the order of 10^{-2} cm or smaller [7]. In particular, in metal-water reaction experiments performed in the Argonne National Laboratory Treat Reactor using Spert I fuel plate samples [8], burning times of the order of 1 sec were observed. The reaction rate in these experiments was found to be very low for temperatures between 1100 and 1600°C, and somewhat higher between 1600 and 1750°C. The reaction rate and extent of burning increased very rapidly for temperatures above 1750° C, which is an apparent threshold temperature. As discussed above, the maximum calculated fuel plate temperature at the core hot spot, assuming an adiabatic temperature rise, is about 1250°C, which is not high enough to produce a rapid reaction rate. The probability of a rapid reaction is further reduced in considering the non-adiabatic fuel plate temperature rise actually obtained,

Assuming that the results of aluminum-water reaction experiments are applicable, then for the explosive pressure developed in Spert I to have been the result of chemical reaction, it would have to be assumed that (a) a portion of the core not only reached temperatures considerably in excess of 1750°C, but also burned at a rate much higher than that previously observed in laboratory experiments, or that (b) the hot fuel was initially fragmented into particles of the order of 10 microns or less in size and dispersed into water. Alternative (b) does not seem reasonable since other mechanisms would be required to cause this initial dispersal of the fuel. The Argonne test results for the Spert I plates and the relatively low fuel temperatures which were actually achieved during the destructive test indicate that for this test the metal-water reaction probably proceeded slowly with a reaction time of the order of seconds and that it occurred as a consequence of the disintegration of the fuel plates caused by the violent steam explosion.

8. METALLOGRAPHIC EXAMINATION OF DAMAGED FUEL PLATES FROM THE DESTRUCTIVE TEST

A metallographic examination has been performed at the MTR hot cell on 8 fuel plates which were melted as a result of the 3.2-msec-period destructive test. The plates and their location in the core are shown in Table I.

TABLE I

METALLOGRAPHIC SAMPLE POSITIONS

Plate No.	Core Position[a]	Plate Position[b]	Approximate Length of Recovered Plate (in.)
D-2321	E-5 (TR)	1	3-1/4
D-2433	E-5 (TR)	12	3
D-1930	E-4	1	8-1/2
D-808	E-4	12	3-3/8
D-800	C-5 (CR)	12	10-3/4[c]
D-2392	C-3	4	25-1/8[d]
D-1163	F-6	6	5
D-365	F-6	7	5

[a] See Fig. 1 for core position nomenclature.

[b] Plates are numbered from west to east within assemblies as positioned in the core.

[c] A bottom portion of the plate was attached to the top portion.

[d] Center of plate was melted.

All samples were 3/4 in. in length and were examined in the unetched state using 50x magnification.

Examination of the composite photomicrograph (Figure 10) for a sample taken at the ruptured end of plate D-2321 reveals the melting of the meat and the cladding. The end is flared, indicating that it had been in a plastic state. Figure 11, which is another photomicrograph of the same sample, but at a position further away from the ruptured end, shows melting at the center and edge of the larger fuel particles, but no damage to the cladding. This sample is a longitudinal-type specimen, ie, the viewing surface is parallel to the long axis of the fuel plate. A transverse-type specimen (Figure 12) from the rupture area shows some melting and change at the edges of the large fuel particles. This sample shows no indication of cladding damage.

The photomicrographs obtained of plate D-2433 are quite similar to those of plate D-2321.

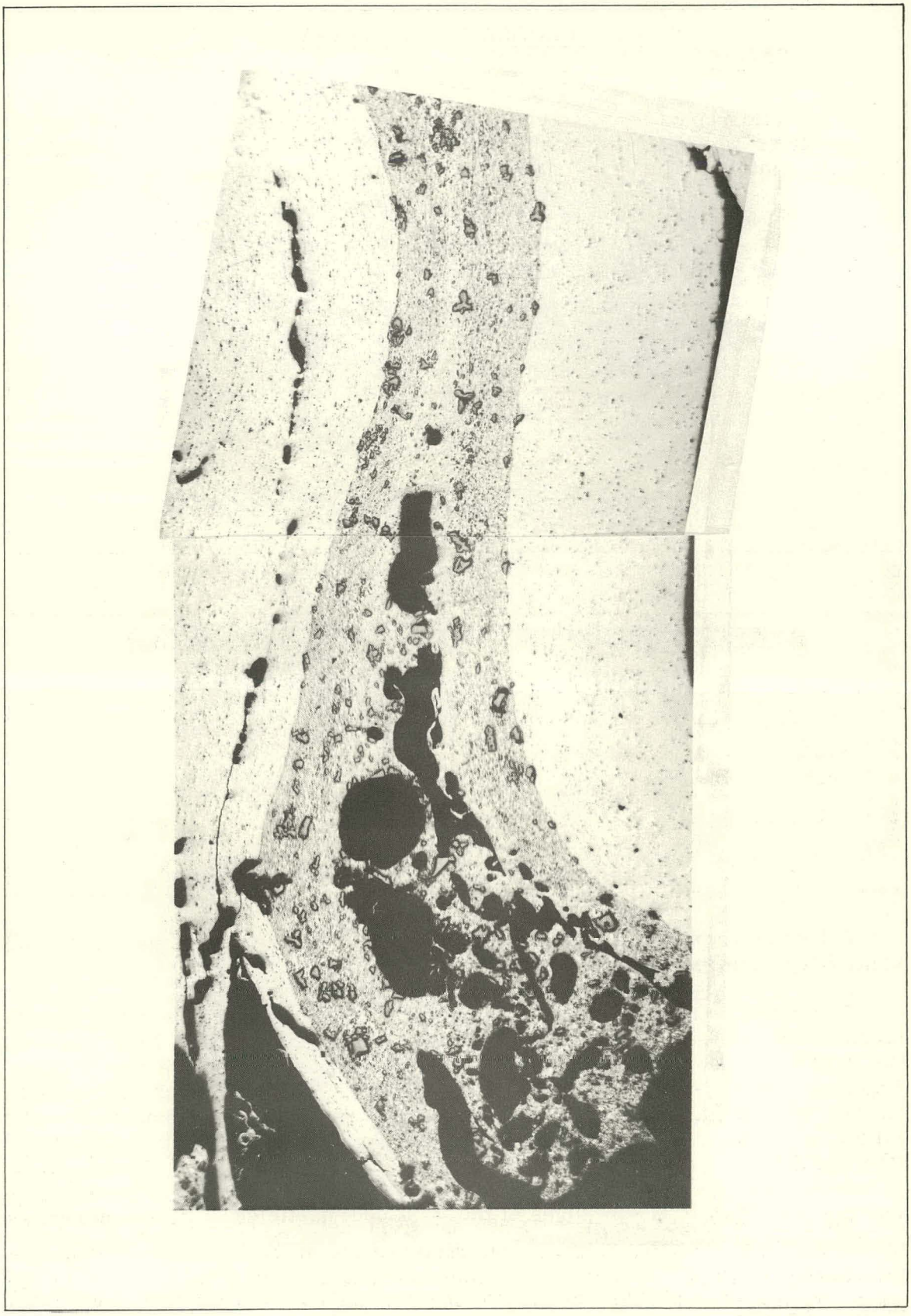

Fig. 10 Composite photomicrograph of ruptured end of fuel plate D-2321 (50x).

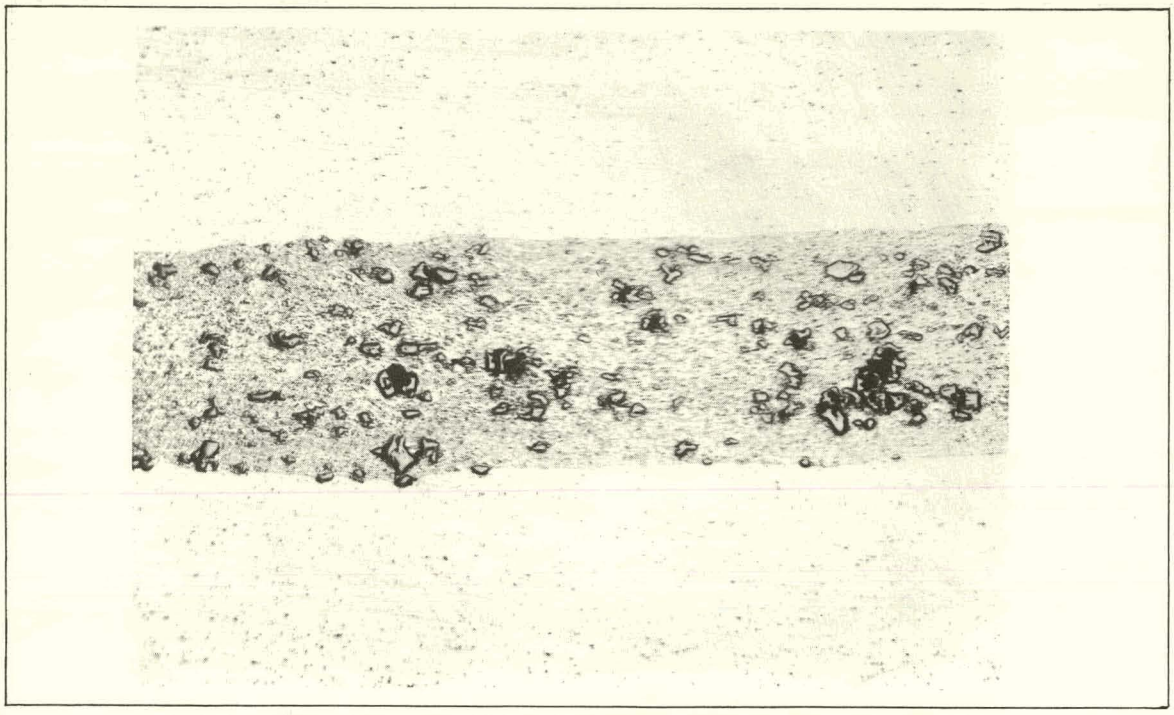

Fig. 11 Photomicrograph of plate D-2321 away from ruptured end (50x).

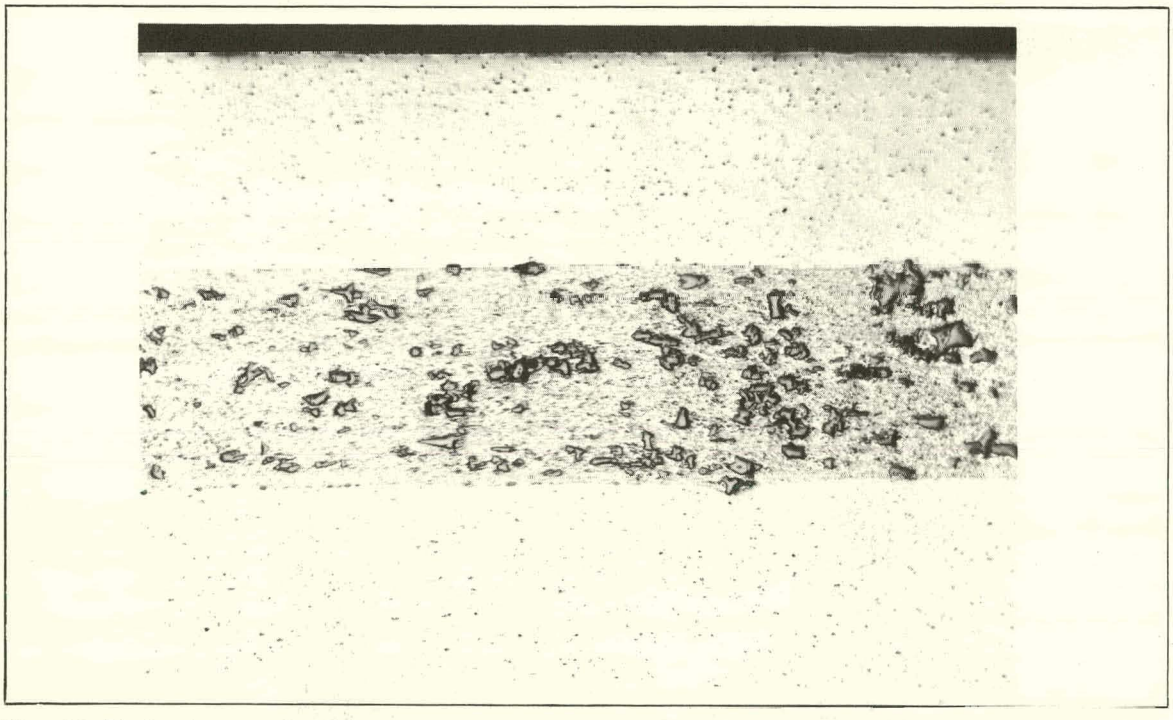

Fig. 12 Photomicrograph of transverse-type specimen from the rupture area of plate D-2321 (50x).

Photomicrographs of plate D-800 show the melting and mechanical damage of the fuel plate. Figure 13 shows the ruptured end of the fuel plate. The photomicrograph of Figure 14 was taken immediately adjacent to that of Figure 13 and shows the cladding damage. Figure 15, which is an area about 3/8 in. away from the area shown in Figure 14, is typical of undamaged fuel samples. A sample from the bottom portion of the D-800 fuel plate is shown in Figure 16. The sample

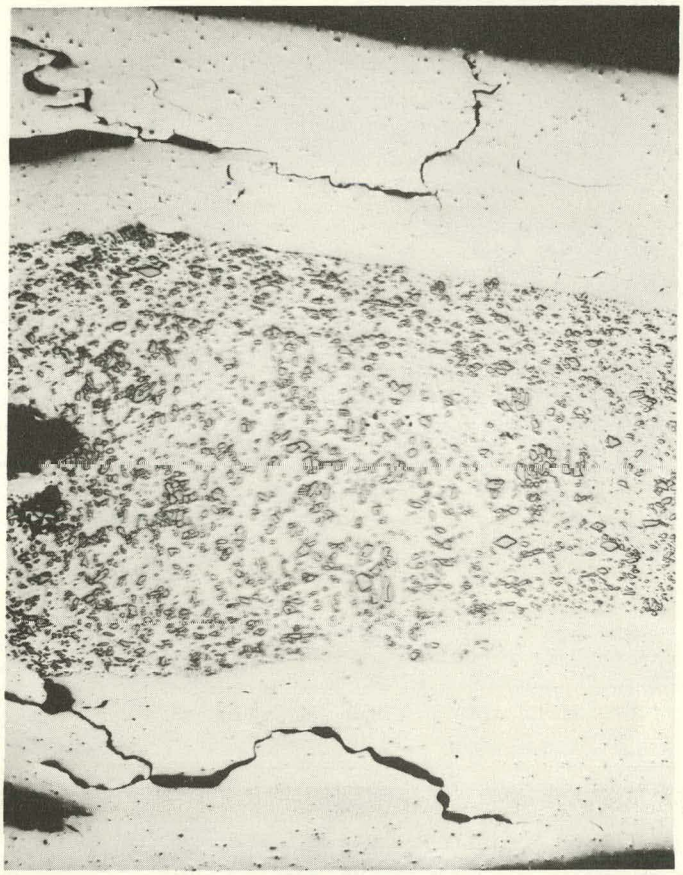

Fig. 13 Photomicrograph of ruptured end of plate D-800 (50x).

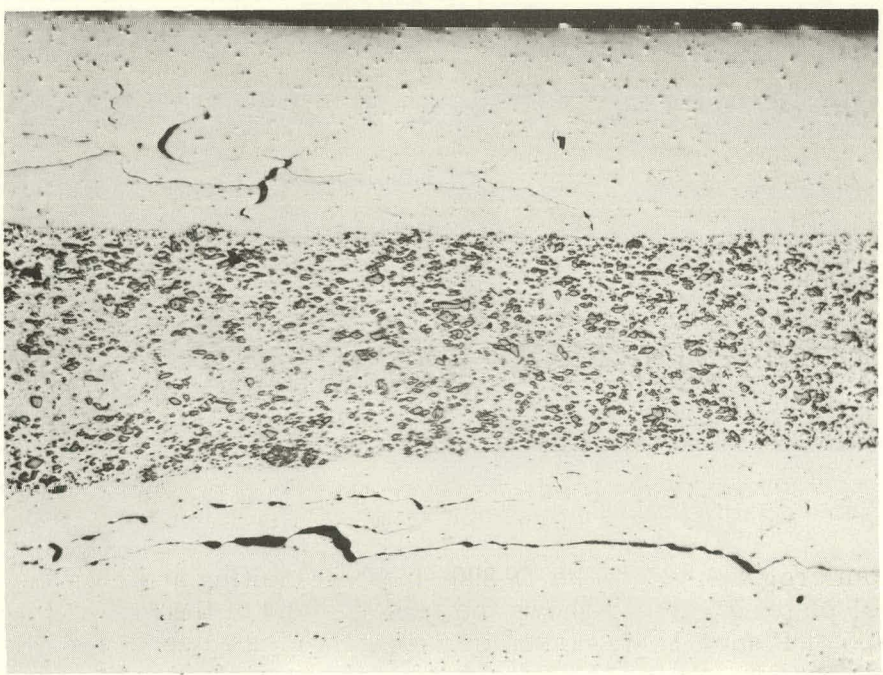

Fig. 14 Photomicrograph of plate D-800. Sample taken immediately adjacent to that of Figure 13 (50x).

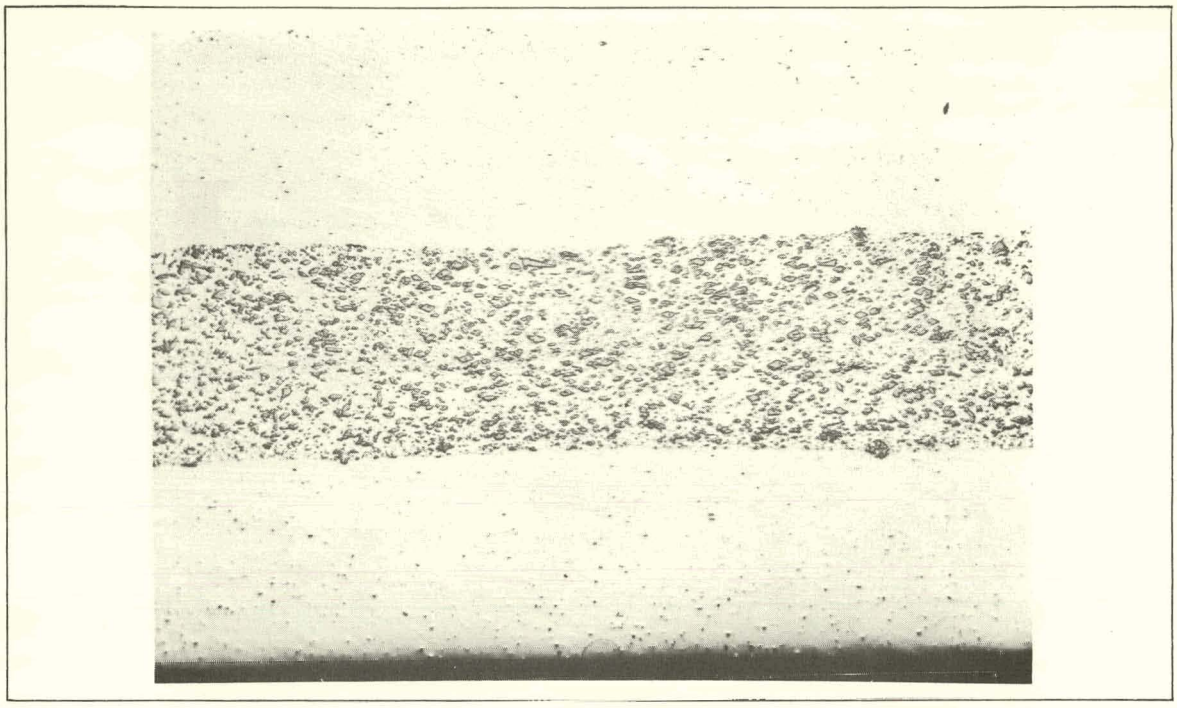

Fig. 15 Photomicrograph of plate D-800. Sample taken about 3/8 in. from that of Figure 14 (50x).

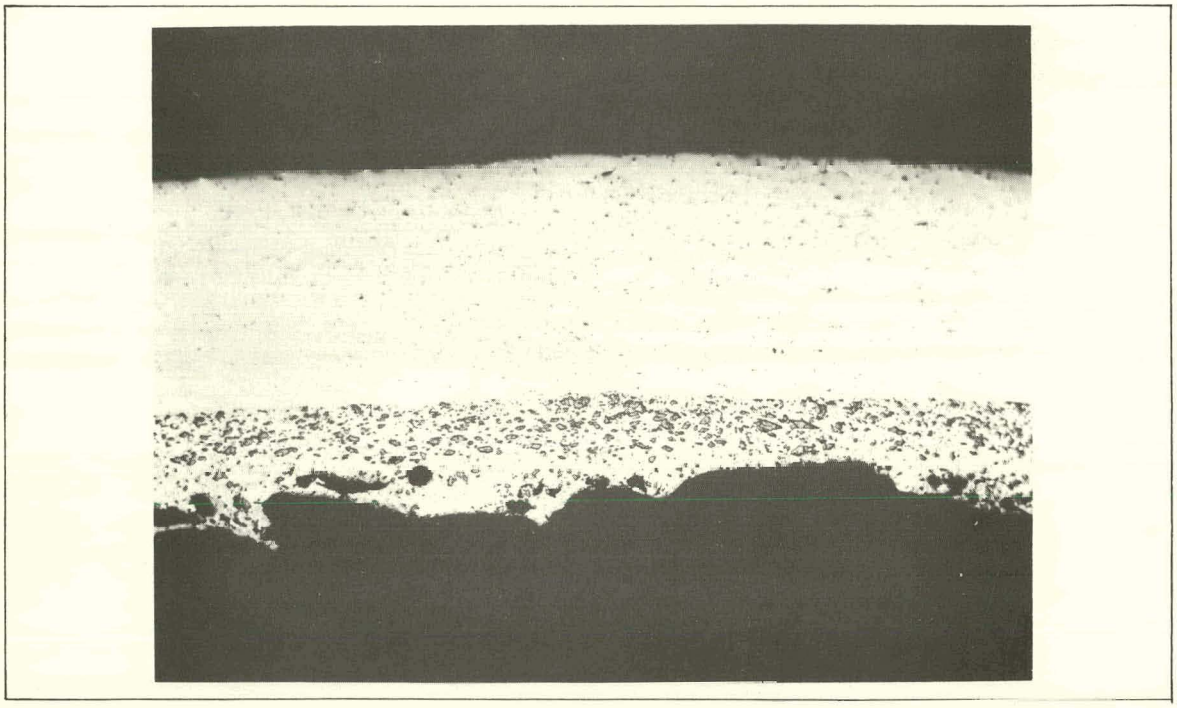

Fig. 16 Photomicrograph of sample from bottom end of plate D-800. Only half of the sample is shown (50x).

exhibits a melted area at the fuel centerline and no cladding damage. The sample split through the fuel before mounting and only one-half of the sample is shown in the figure.

Figure 17 shows a sample of plate D-808 near the ruptured end. In this case the cladding is severely cracked, and the meat shows some centerline fuel out-

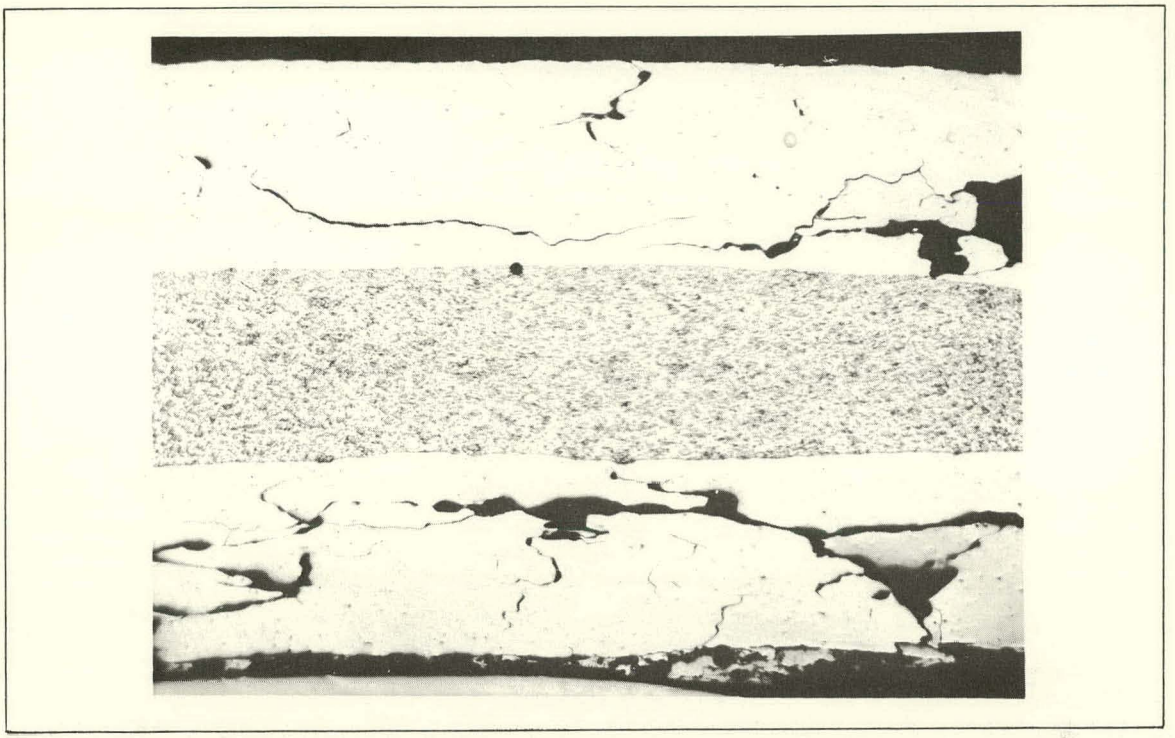

Fig. 17 Photomicrograph of sample near the ruptured end of plate D-808 (50x).

lining. A sample which was taken 2 in. from the ruptured end shows no apparent melting.

Samples from plate numbers D-1930, D-1163, and D-365 exhibited characteristics similar to the samples from plate D-808.

Samples taken at 5-1/2, 10, 13-1/8, and 16-3/8 in. from the top of fuel plate D-2392 were examined. The 5-1/2- and 10-in. samples show typical areas with no melting. The 13-1/8- and 16-3/7-in. samples show no cladding damage and some outline melting of the larger fuel particles (Figure 18). Since the 13-1/8- and 16-3/8-in. samples were taken from the damaged area of the plate, it is somewhat surprising to see so little evidence of melting.

In general, the melting of the fuel plates on the damaged ends extended into the plates about 1/8 in. At about 3/8 in. from the ends, or in the middle of the specimens taken from the damaged ends, normal fuel plate structure was observed. In a very few samples, damage was observed in areas away from the melted end.

The failure of the fuel plates can be described as a combination of melting and mechanical damage. The observed intergranular cracking of the cladding and the melting of the meat near the ruptured ends shows that the plates must have reached a temperature of at least 640°C in this vicinity. Because of the absence of cladding and meat damage a short distance from the damaged end, it appears that the temperature gradient was large along the length of the plate. While this evidence, coupled with a temperature reading of 1230°C from the fuel-bearing capsule (see above) which was in the core, indicates that the temperature of the fuel plates was probably much higher than that recorded by surface thermocouples; there is no metallographic evidence that the maximum fuel temperatures approached the vaporization temperature of the alloy.

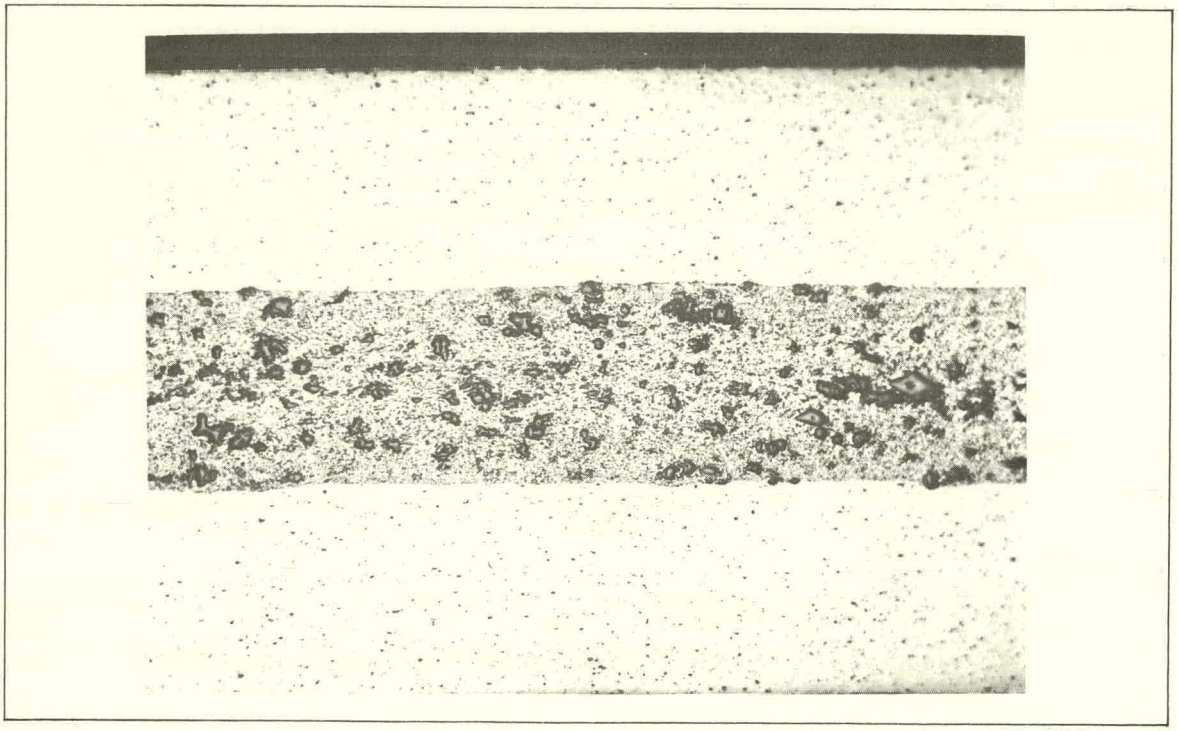

Fig. 18 Photomicrograph of sample from plate D-2392 (50x).

A more detailed presentation and discussion of metallographic data for the destructive test fuel is contained in a report in preparation [4].

9. PREPARATIONS FOR FUTURE TESTS

During the present quarter, the cleanup and recovery operations described above were completed, and restoration, repair, and modification of the Spert I facility for the next test series were initiated.

A program of non-destructive excursion tests was previously performed in the Spert I facility with a low-enrichment oxide-rod-type core[9,10]. The next experimental program to be pursued in the Spert I facility will be a series of tests leading to the destruction of the oxide core previously investigated. The core structure, control rods, and rod drive extensions utilized in the earlier oxide core tests have been adapted, and are presently being installed in the 10-ft-diameter Spert I vessel.

The combination of the long thermal time constant in this fuel and the Doppler mode of reactivity shutdown has, in the previous tests of the oxide core, resulted in insignificant transient pressures being developed for excursions with periods as short as 3.2 msec. It is expected however, that as shorter-period tests are performed in the forthcoming test series, thermal stresses in the cladding and/or expansion of the UO_2 will ultimately cause cladding rupture, with the consequent sudden release of the finely divided UO_2 powder into the reactor water. This will result in a sudden increase in rate of energy deposition in the water, which may produce larger destructive effects than those observed in the recent plate-

type destructive test in Spert I. The primary objective of the forthcoming program will be to determine the nature of the destructive effects produced when the high-energy-content UO_2 is dispersed into the reactor water as a result of cladding failure during a power excursion. It is estimated that, utilizing the fuel, core structure, and control system presently available, the shortest-period test which can be performed ($\approx$ 2 msec) will produce a nuclear energy release of about 200 Mw-sec. If it is found that a single such test does not produce fuel rod rupture in this core, tentative plans call for attempts to produce the desired rupture by repeated short-period tests, and/or by placement of purposely defective fuel rods in the central region of the core.

There is a recognized need for subassembly investigations of the nature of the rapid meltdown of highly enriched fuel plates of various designs, in order to further the understanding of the plate-type destructive test results and their application to other plate-type cores. For this reason, it is planned to obtain such data on a limited basis by means of instrumented fuel capsules which can be installed in the reflector region around the core during the forthcoming transient tests on the oxide core.

By the end of the first quarter of 1963, preparation of the Spert I facility for the oxide-core destructive test program, including repair of cracks in the reactor vessel, resealing of the concrete floor of the tank, and cleaning and painting of the tank had been completed. Design of the necessary mechanical modifications to the reactor system also had been completed, and fabrication and installation of the core components was underway.

II. SPERT IV

1. INTRODUCTION

A series of tests has been initiated to determine the response of the Spert IV, plate-type core to a step input of reactivity at ambient temperature, for various initial system conditions of hydrostatic head above the core and forced-coolant circulation rate. During the first quarter of this year the following excursion tests were completed: tests in the period range from 1 sec to 8.5 msec, with an 18-ft hydrostatic head above the core and no forced circulation; tests of approximately 20-, 12-, and 8.5-msec-periods, with a 2-ft hydrostatic head and no forced coolant circulation; and tests in the period range from approximately 500 to 10 msec, with an 18-ft hydrostatic head and with a forced-coolant circulation rate of 5000 gpm (12 ft/sec) through the core. Further testing at different forced coolant rates is planned for the second quarter of this year.

The following discussions include descriptions of the kinetic behavior of the reactor power, energy, fuel plate surface temperature, and transient pressure during the tests, and of a determination of the reduced prompt neutron lifetime deduced from the test results. The results which are presented in these discussions are preliminary; however, it is not expected that the final results will deviate significantly from the values presented.

2. FIDUCIAL TRANSIENT TESTS FOR 18-FT HEAD

In order to establish the transient behavior of the Spert IV core under natural circulation conditions and to provide reference data with which to compare results of tests under other initial conditions, a series of step-induced, power excursion tests was performed for the period range from approximately 1 sec to 8.5 msec. The hydrostatic head above the core was approximately 18 ft (the maximum available for the core as presently installed) and the bulk water in the reactor vessel was at ambient temperature. Tests with periods longer than about 15 msec were initiated with the reactor power at approximately one watt. Tests with shorter periods were initiated from a few milliwatts, in order that the reactivity insertion could be completed before a significant power rise occurred.

The reactor power behavior during these tests was very similar to that observed during previous test series with various other cores at Spert. In general, the reactor power rises exponentially until the energy released during the excursion, acting through various reactivity-compensating mechanisms, causes the power to self-limit and seek a lower equilibrium value. Most of the tests were terminated before the equilibrium power had been clearly established. The peak powers reached during these tests as a function of initial reciprocal period, α_o, are shown in Figure 19. Figure 20 shows the power, fuel plate surface temperature, and transient pressure during a test with an asymptotic period of 8.5 msec. This is the shortest-period test that has been performed thus far in the test series.

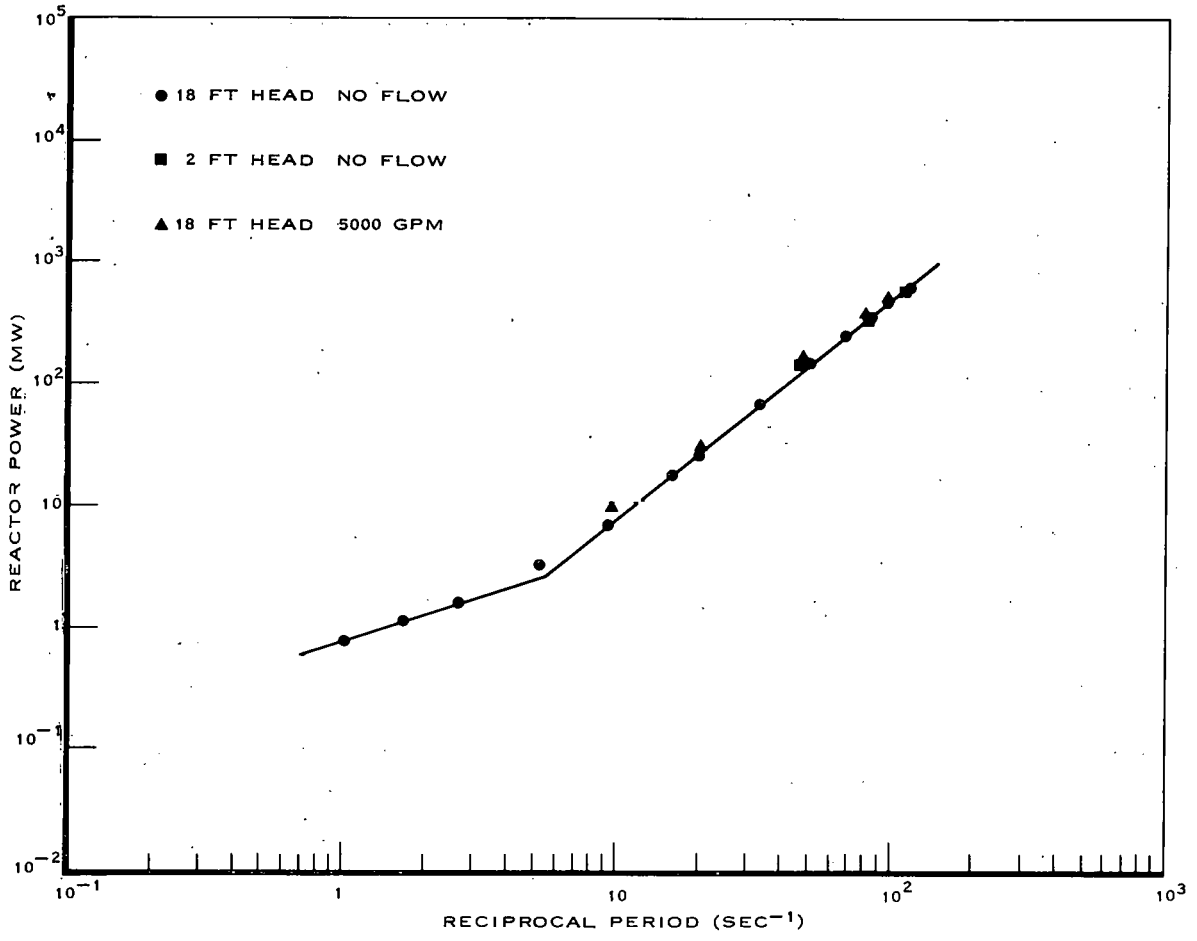

Fig. 19 Peak power vs reciprocal period for Spert IV tests with 18-ft head.

The energy released during the tests in this series was obtained by integration of the power traces. In general, the energy released up to the time of the power peak was found to decrease over the range of reciprocal periods from 1 to 6 sec^{-1} and thereafter to increase with increasing α_o. The energy released up to the time of peak power is shown as a function of α_o in Figure 21.

Fuel plate surface temperatures were measured at 24 representative points in the core by chromel-alumel thermocouples fabricated from 10-mil-diameter wires, with the junction flattened to about 3 to 4 mils and spot-welded to the fuel plates.

Data showing the fuel plate surface temperature at the time of the power peak, and the maximum temperature recorded, as functions of α_o are shown in Figures 22 and 23, respectively. These data were obtained from a thermocouple which usually indicated the highest temperature of any thermocouple in the core. It was located 4 in. below the core centerline on one of the central fuel plates in the central transient rod assembly.

It can be observed from Figure 22 that only non-boiling shutdown mechanisms (moderator heating, fuel plate expansion, etc) are required to limit the power rise for tests with $\alpha_o < 20$ sec^{-1}, since the boiling point (about 109°C at the core

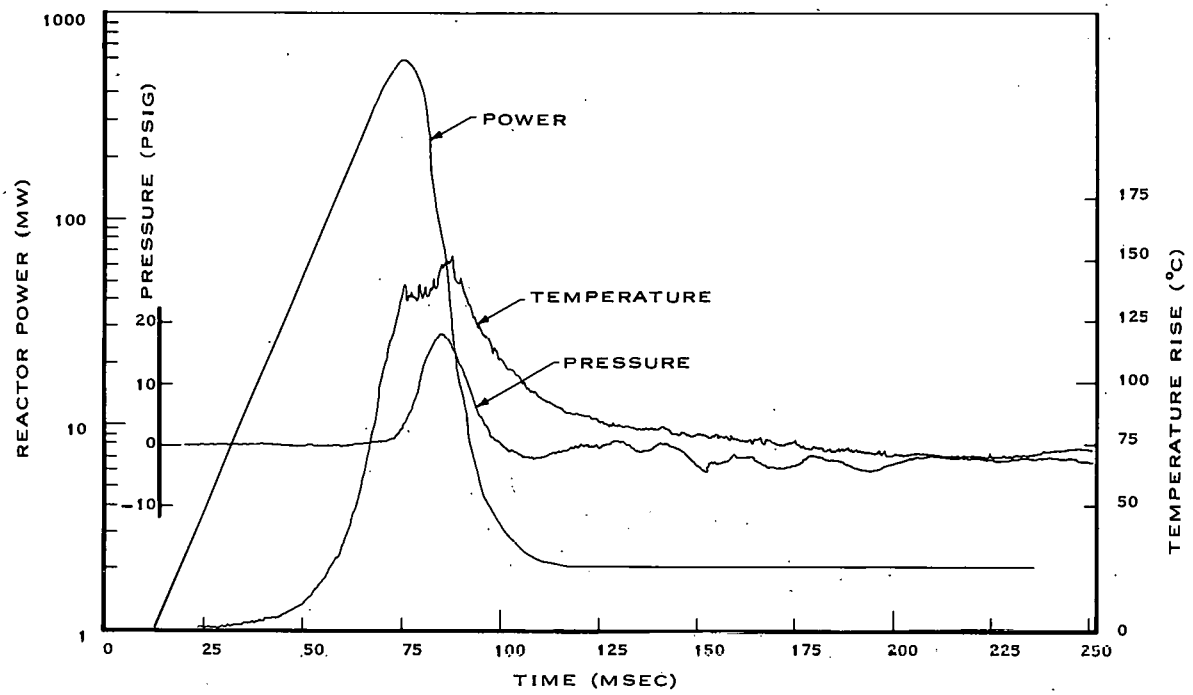

Fig. 20 Reactor power, fuel plate surface temperature, and transient pressure for 8.5-msec-period test with 18-ft head, no flow.

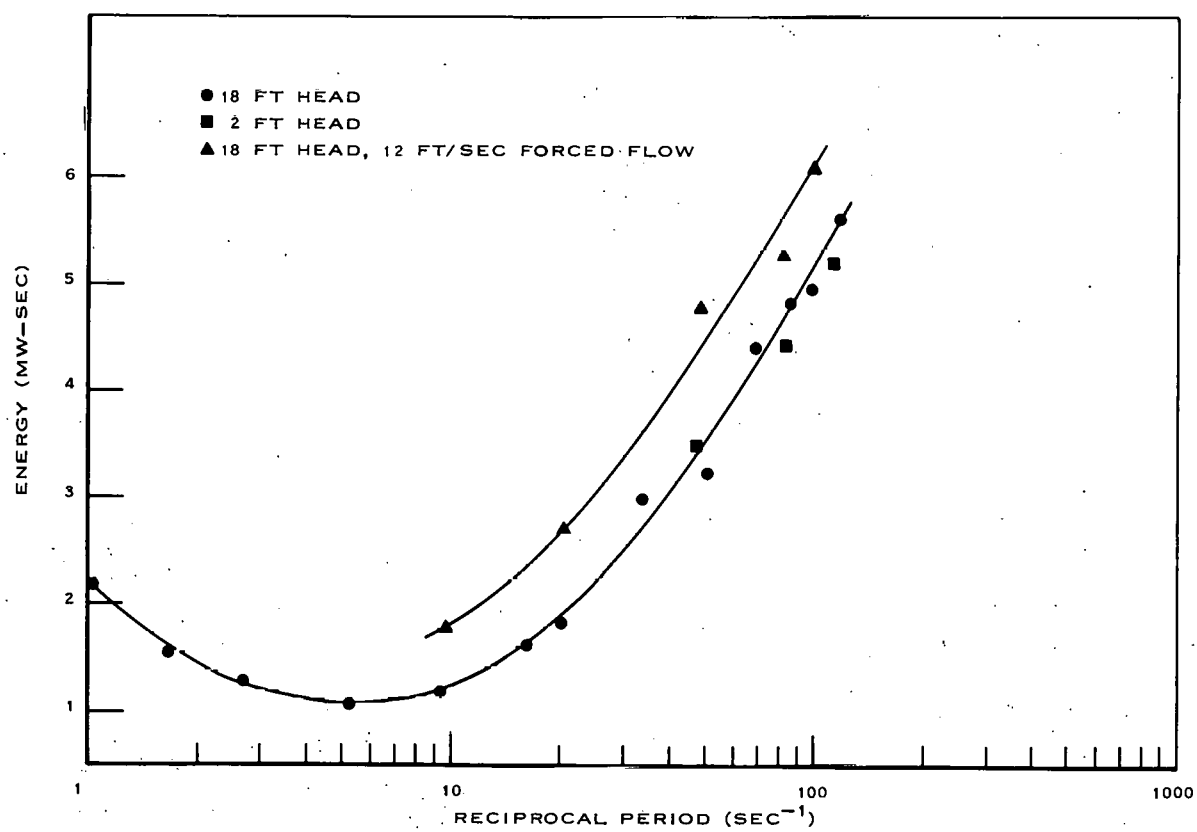

Fig. 21 Energy release at time of peak power vs reciprocal period for various water head and flow conditions.

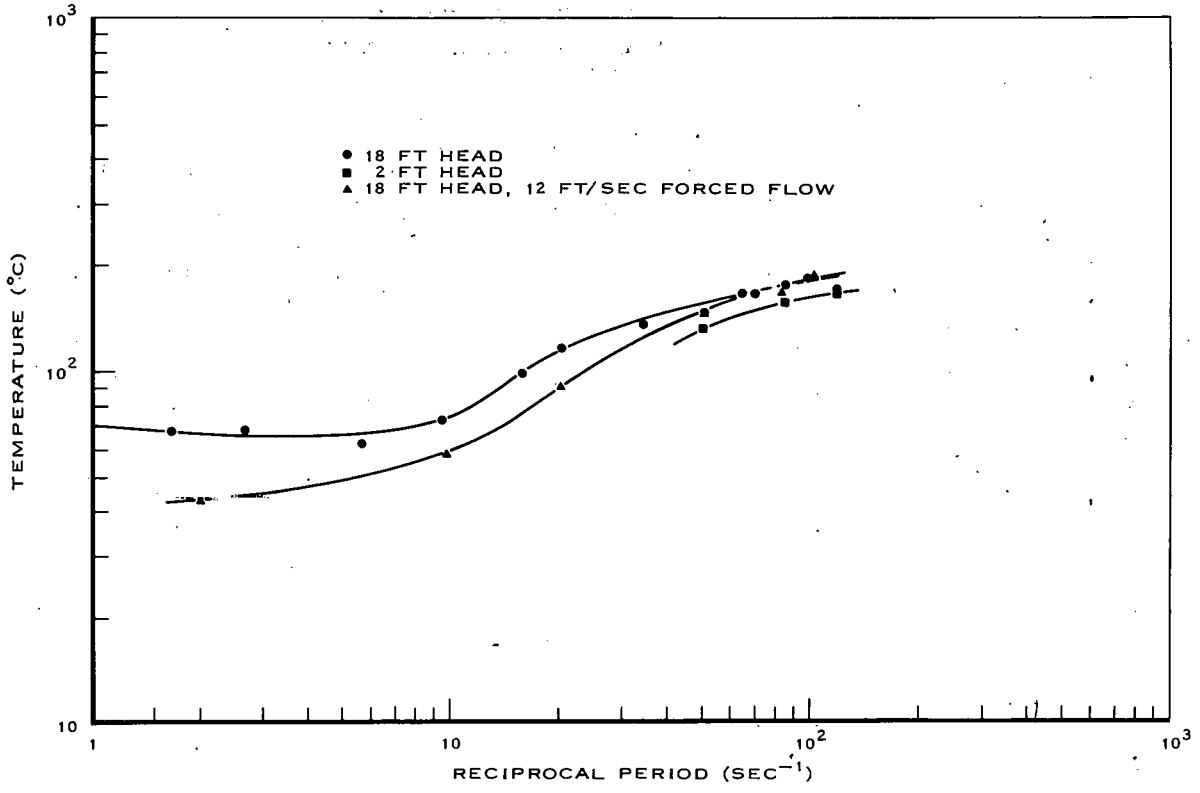

Fig. 22 Fuel plate surface temperature at time of peak power vs reciprocal period for various water head and flow conditions.

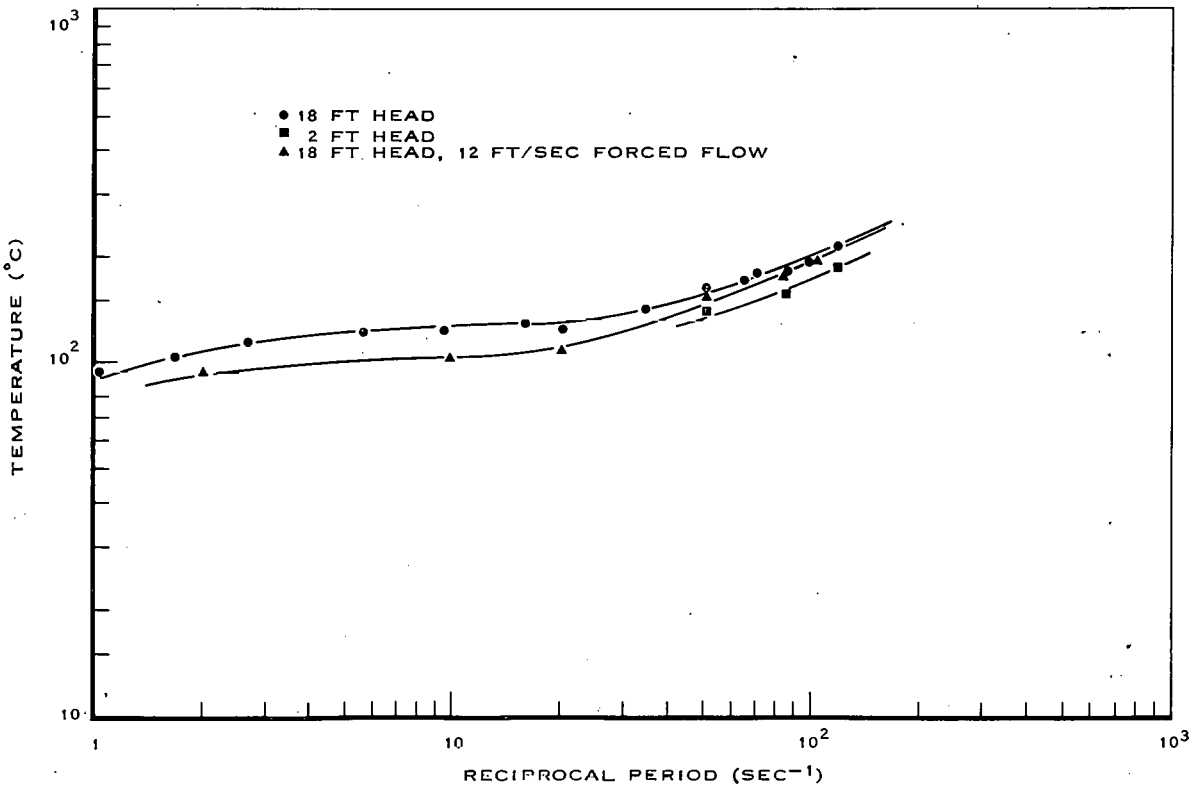

Fig. 23 Maximum fuel plate surface temperature vs reciprocal period for various water head and flow conditions.

centerline with an 18-ft head of water) was not reached at peak power for those tests. However, as α_o increases beyond this value, steam void formation becomes an important shutdown mechanism.

The maximum fuel plate surface temperatures, shown in Figure 23, are below or only slightly above the boiling point for $\alpha_o < 20$ sec^{-1}, indicating that for this period region boiling heat transfer is adequate to prevent appreciable superheating of the fuel plates. For values of α_o greater than 20 sec^{-1}, however, the maximum surface temperatures increase with α_o. The rise in maximum temperature as period is decreased is thought to be a result of partial "vapor blanketing". With the attainment of temperatures much above the boiling point, steam vapor blanketing, which decreases the heat transfer rate from the fuel plate allowing the temperature to increase rapidly, can be established early in the power excursion.

During this series of tests, the transient pressure generated during the excursions was measured using unbonded-strain-gauge type transducers positioned as shown in Figure 24. Useful data were obtained only from transducers at

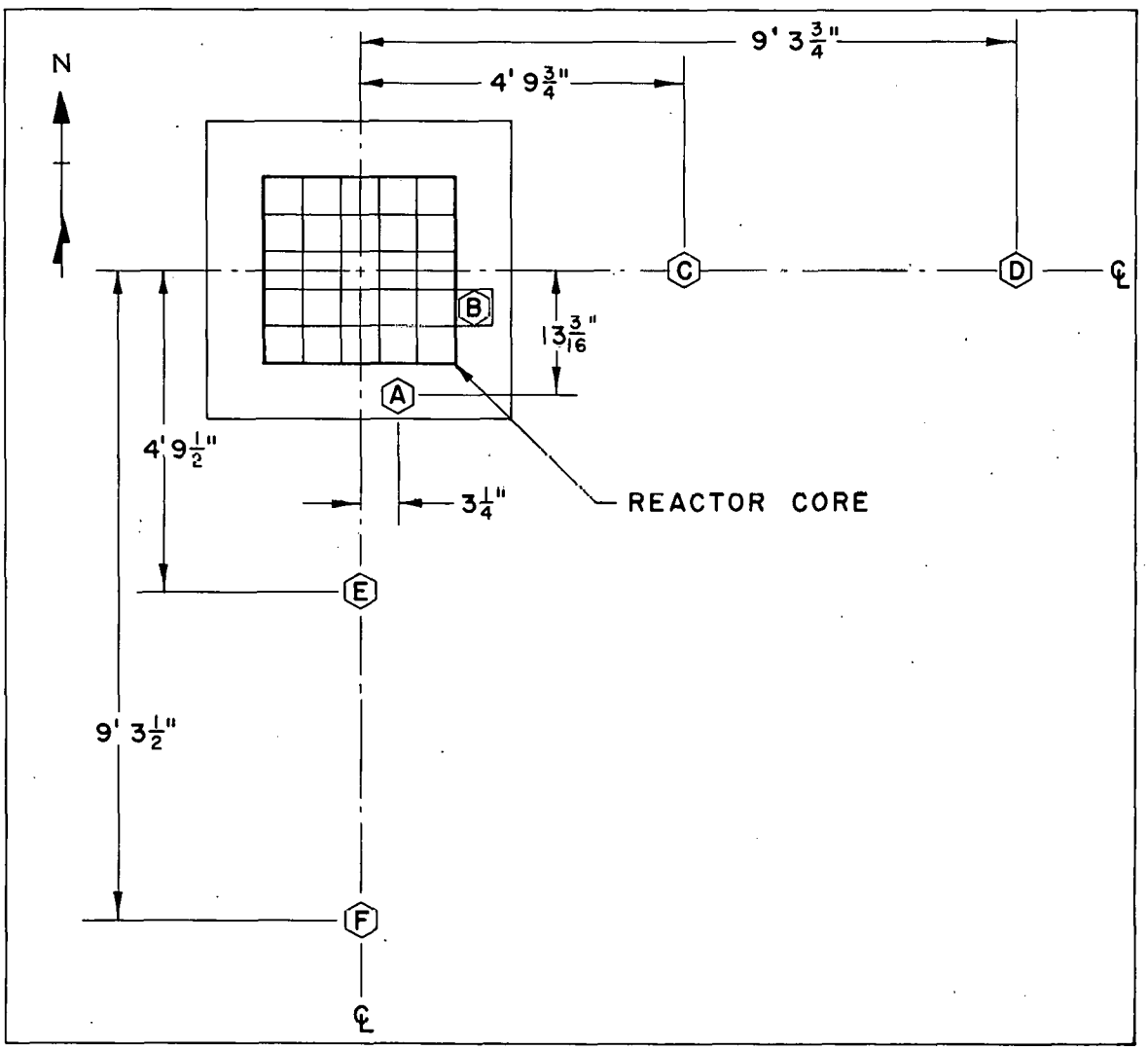

Fig. 24 Locations of pressure transducers around Spert IV core. (Transducer "A" located 26-5/16 in. below core centerline; all others located at centerline.)

positions "A" and "B" nearest the core, the other positions being too remote to experience measurable pressure pulses, even for the 8.5-msec-period test.

The pressures recorded beneath the core at "A" were the result of the downward expulsion of water from the core arising from the rapid increase in temperature during the transient. The pressure detected at this position was characterized by damped oscillatory behavior as is shown in Figure 20. The transducer at "B" was mounted in a dummy fuel assembly can loaded in a core position adjacent to the core. The pressures recorded here were small compared with those at "A", since mass movement of water in the horizontal direction is restricted by the fuel assembly cans. The "B" transducer recorded the small pressure pulse transmitted horizontally through the core, superimposed on the response of the transducer to the vibration of the assembly in which the transducer was mounted.

Figure 25 is a plot of the peak pressures measured at both "A" and "B" versus α. Included on this plot are pressure data taken for all transient tests which have been performed thus far including those with forced coolant circulation.

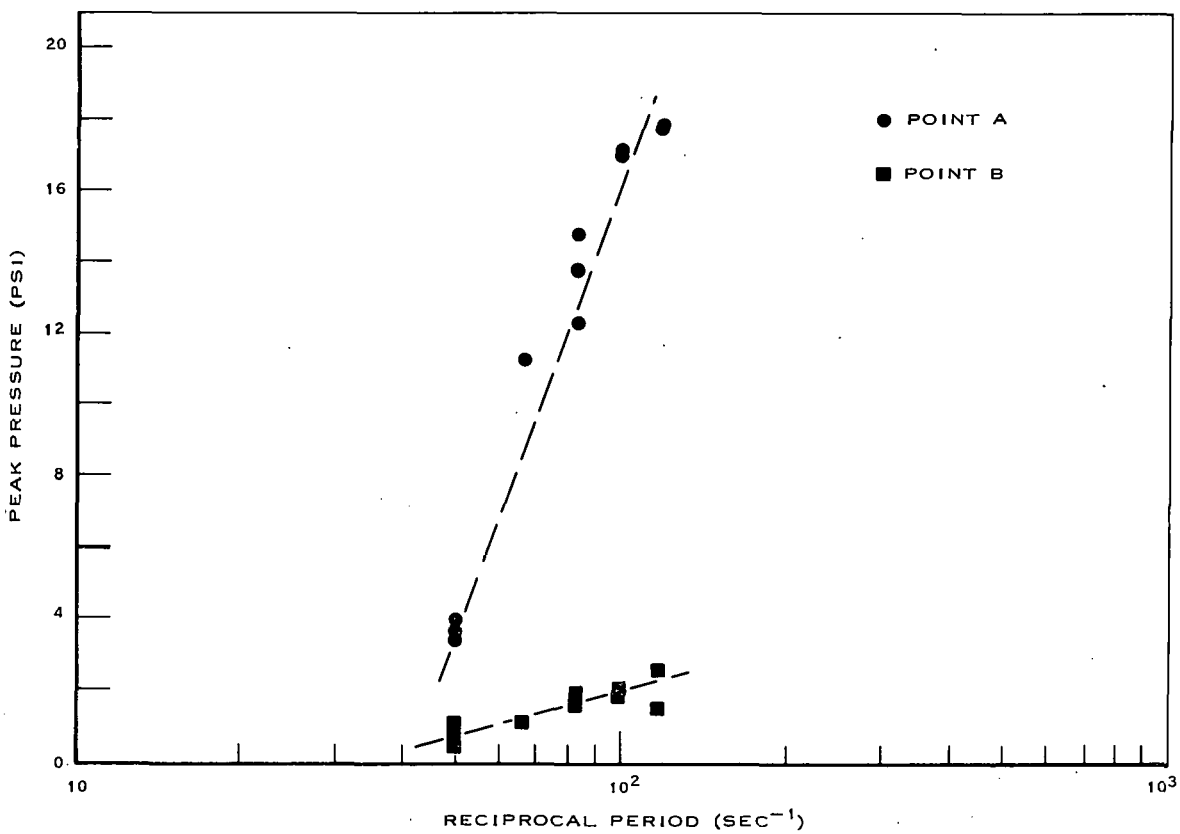

Fig. 25 Peak transient pressure vs reciprocal period.

3. EFFECT OF DECREASED HYDROSTATIC HEAD

A short series of tests was performed to investigate the effect of variations in hydrostatic head on the response of the Spert IV reactor to stepwise reactivity additions. In this investigation, the water head above the core was reduced from 18 to 2 ft and tests with asymptotic periods of 20, 12, and 8.5 msec were performed. These tests were limited to the short-period region where boiling is a significant shutdown mechanism and where the change in hydrostatic pressure of 6.9 psi (change in boiling point of 14°C) should produce the greatest change in the reactor response. The following results were observed for these tests.

(1) There was no significant change observed in the peak power, burst shape, or energy release as a result of the lowering of the hydrostatic head. For the shortest-period test that was performed for both head conditions (≈ 8.5 msec), the peak power for the 2-ft-head test was only about 6% lower than for the 18-ft-head test.

(2) The fuel plate surface temperatures at the time of peak power were about 20°C higher and the maximum temperatures were about 25°C higher in the 18-ft-head tests than in the 2-ft-head tests.

(3) The data were insufficient to draw any firm conclusion concerning the change in transient pressure behavior as a result of the hydrostatic head change. Of the tests performed, only the 12-msec-period test showed any significant difference, the transient pressure measured beneath the core being about 20% higher for the 18-ft-head test.

These results can be compared with results from previous tests involving a change in hydrostatic head or initial system pressure which have been performed in the other Spert reactors.

A series of transient tests was previously performed in Spert I with the A-17/28 core for both a 2-ft and 9-ft hydrostatic head above the core [11]. There was essentially no difference in the test results for the tests initiated at ambient temperatures. For the tests initiated with the bulk-water temperature at boiling, however, the peak power reached in the 9-ft tests were approximately a factor of two higher than for the 2-ft tests and the power bursts were considerably broader for the higher head tests.

A series of ambient temperature tests was previously performed in Spert III in which the initial system pressure was raised from atmospheric to 2500 psig [12]. Results from these tests showed that for the shorter-period tests where boiling is a significant shutdown mechanism at atmospheric pressure, the peak powers were increased by approximately 30% as the pressure was increased to 2500 psig, with most of the change occurring in the first 50 psi of pressure increase. Also, in the higher-pressure tests, the power burst shape was somewhat broadened, with a consequent increase in the energy release.

Transient pressure measurements which have been made during power excursions initiated at atmospheric pressure and at elevated system pressures in Spert II and Spert III have shown that an increase in initial system pressure up to

approximately 75 psig causes increases in the transient pressures observed. With further increases in initial system pressures, the transient pressures either cease to increase or decline, depending on whether the system has room for liquid expansion.

In general, the results of a limited amount of data from the investigation of the hydrostatic head effect in Spert IV are in agreement with the results from the other reactors. In particular, it was found that raising the hydrostatic head above the core from 2 to 18 ft had no significant effect on reactor behavior for excursions initiated at ambient temperature.

4. THE EFFECT OF FORCED COOLANT CIRCULATION

A series of tests has been initiated to investigate the effect of forced coolant circulation on the transient behavior of the Spert IV core. The tests which were completed this quarter were performed over the range of asymptotic periods from approximately 500 to 10 msec with a forced-coolant flow rate of 5000 gpm (12 ft/sec) through the core and with an 18-ft hydrostatic head above the core. This is the maximum available flow rate for the Spert IV facility. The results of previous tests performed in the Spert III facility with up to 18 ft/sec flow through the core [13] showed that for long-period excursions the initial power peak tended to be eliminated as forced flow rate was increased, but for tests with periods shorter than about 50 msec, the addition of flow did not appreciably affect the initial peak. For all the Spert III tests, the equilibrium power level following the initial power rise increased approximately proportionately with the flow rate. This same general behavior has been observed for the tests which have been completed to date in Spert IV.

In the long-period region, where the dominant shutdown mechanisms are fuel plate and moderator expansion, the addition of 12-ft/sec flow results in a substantially different power behavior. Figure 26 shows the power behavior for tests both with and without forced flow in the period region of 500 to 600 msec. The power in the test with forced flow shows no initial peak, but initially rises to about 10 Mw then breaks into small oscillations and continues to rise to about 20 Mw. The test with no flow, however, shows a definite peak of about 1 Mw, followed by an equilibrium power level of approximately one-half megawatt.

For forced-flow tests with periods shorter than about 100 msec, the power exhibits an initial peak which is higher than for the corresponding test without flow for all periods down to 10 msec, which is the shortest period for tests performed thus far with flow. The difference, however, decreases as the period is shortened.

The post-burst power behavior with flow is characterized by a series of damped secondary power bursts. As the initial reactor period becomes shorter, steam formation becomes a more dominant shutdown mode and the magnitudes of the secondary power oscillations become larger with shorter reactor periods, because the growth and collapse of steam bubbles following the initial power burst cause larger changes in reactivity. The frequency of oscillation of the secondary power bursts varies from about 2.5 per second for the 50-msec-period test to about 5 per second for the 10-msec-period test. The secondary oscillations

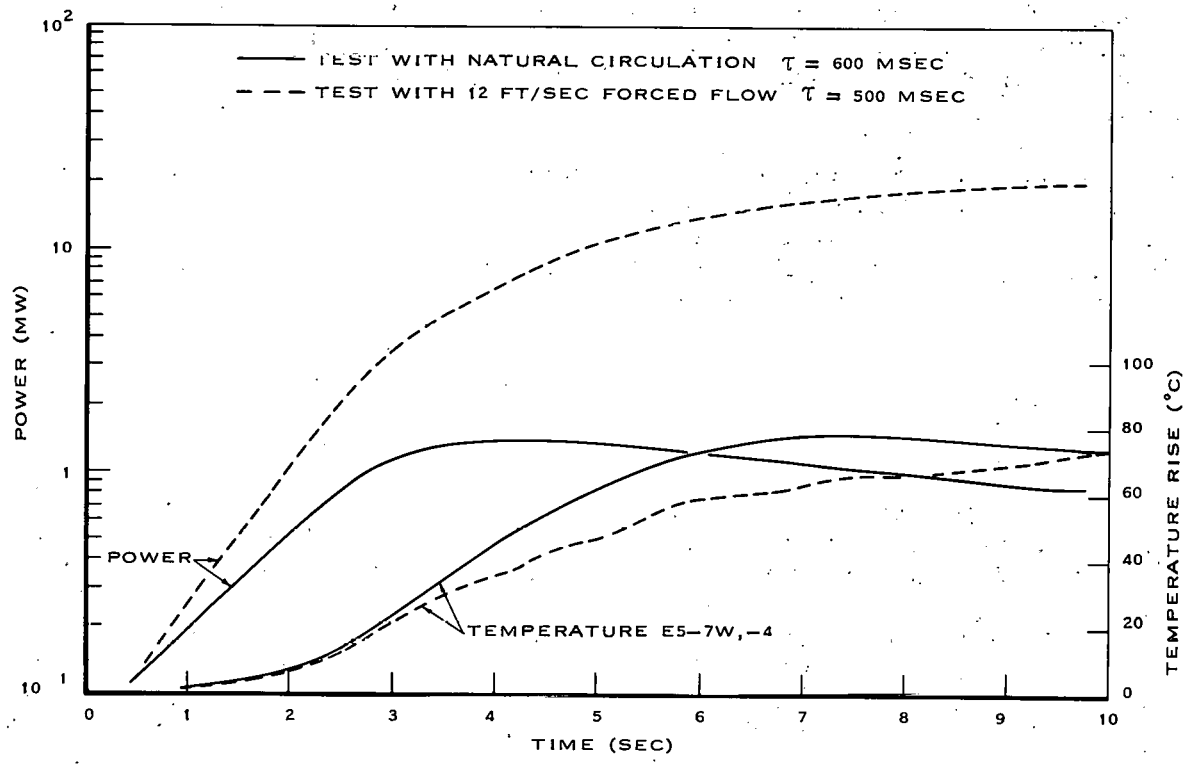

Fig. 26 Reactor power and fuel plate surface temperature as functions of time for long-period excursions with and without forced coolant flow.

appear to seek an equilibrium power level which is about 20 Mw for medium-period tests, and increases to about 30 Mw as the period is shortened.

Figure 27 shows reactor power as a function of time for the 10-msec-period excursion test, the shortest-period flow test performed. Figures 28, 29, and 30 are comparison plots of reactor power vs time for a number of tests involving both flow and no-flow conditions.

Although higher powers were reached with flow, the addition of a 12 ft/sec forced coolant flow resulted in lower values for the maximum fuel plate surface temperatures reached and for the temperatures at time of peak power, than those which were observed during the tests without flow for values of α_o less than about 30 sec^{-1}. For values of α_o greater than 30 sec^{-1}, however, the flow had little effect on these temperatures. This type of behavior is to be expected since, for example, in a 10-msec-period test, the coolant moves only about 3 in. during the time that the reactor power increases by a factor of ten.

The fuel plate surface temperature at the time of peak power and the maximum temperature measured are shown in Figures 22 and 23, as functions of α_o.

Since the addition of forced flow resulted in higher peak powers and slightly broader burst shapes, it would be expected that the energy releases would increase also. The energy release up to the time of peak power for the tests with flow was about 50% higher than for the no-flow case for an α_o of approximately 10 sec^{-1}, and decreased to about 15% higher for an α_o of 100 sec^{-1} (see Figure 21).

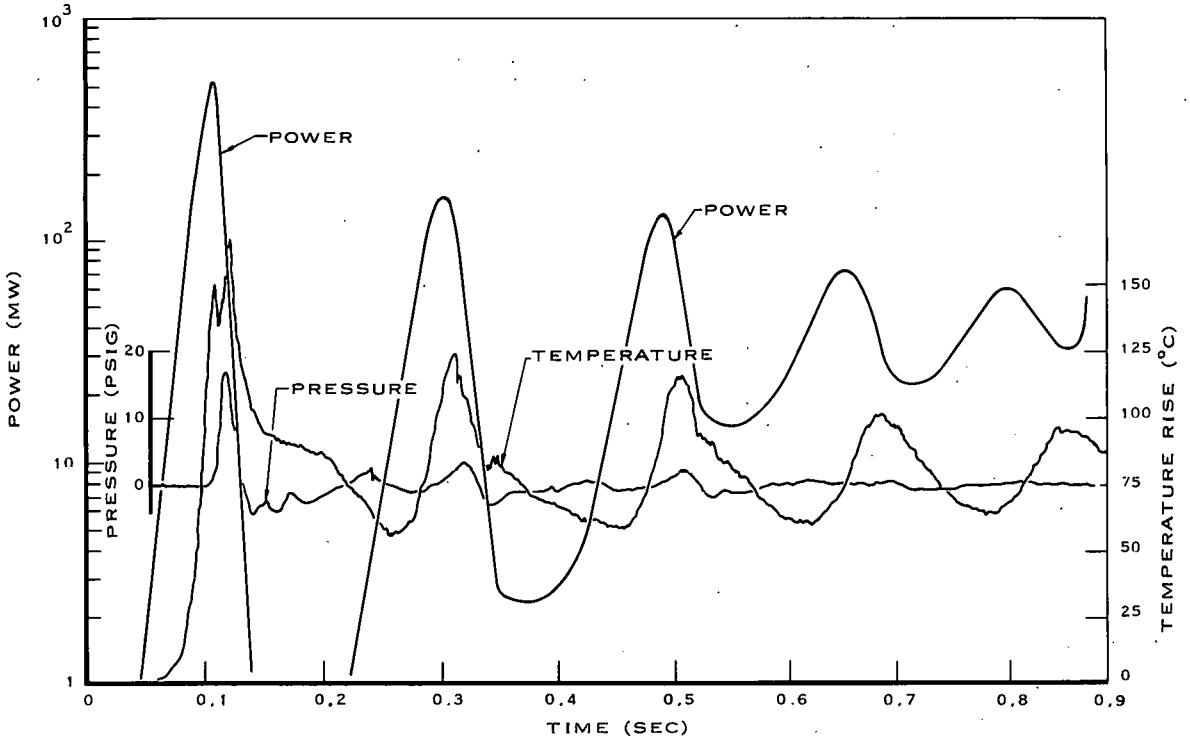

Fig. 27 Reactor power, fuel plate surface temperature, and transient pressure for 9.7-msec-period test with 12 ft/sec forced flow.

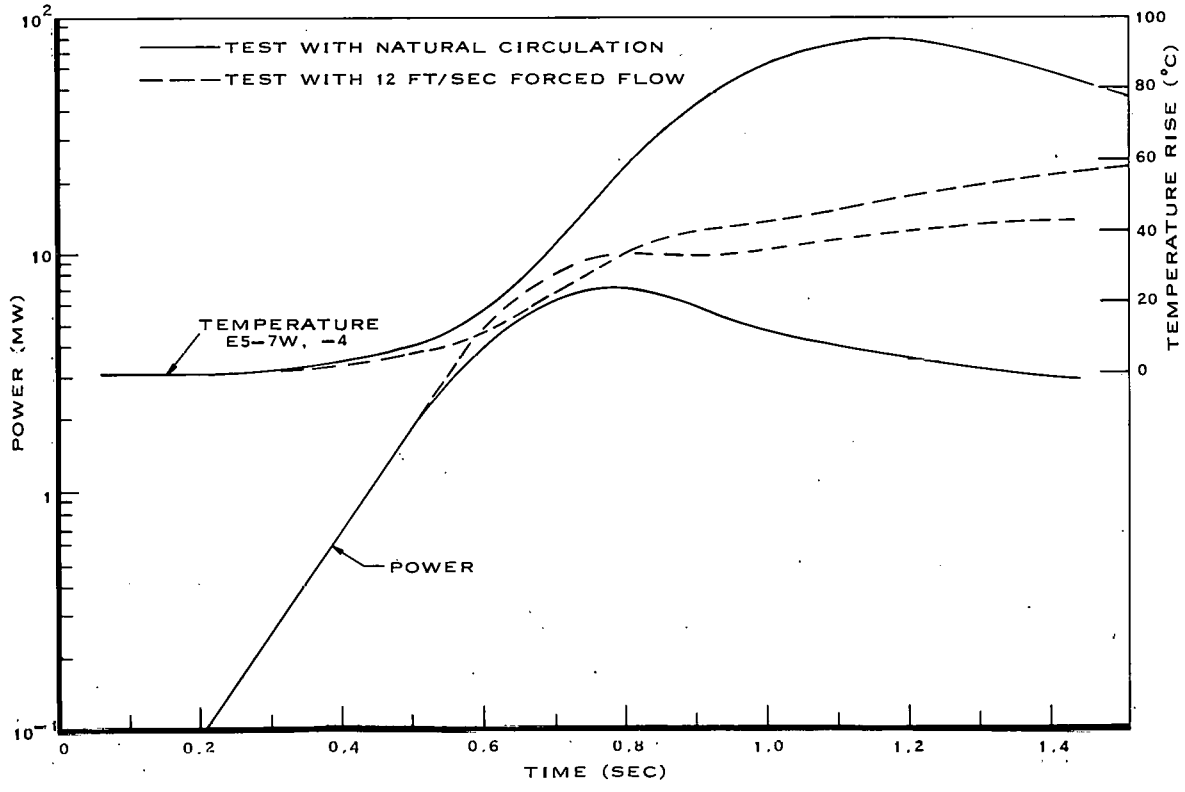

Fig. 28 Reactor power and fuel plate surface temperature for 100-msec-period tests with and without forced coolant flow.

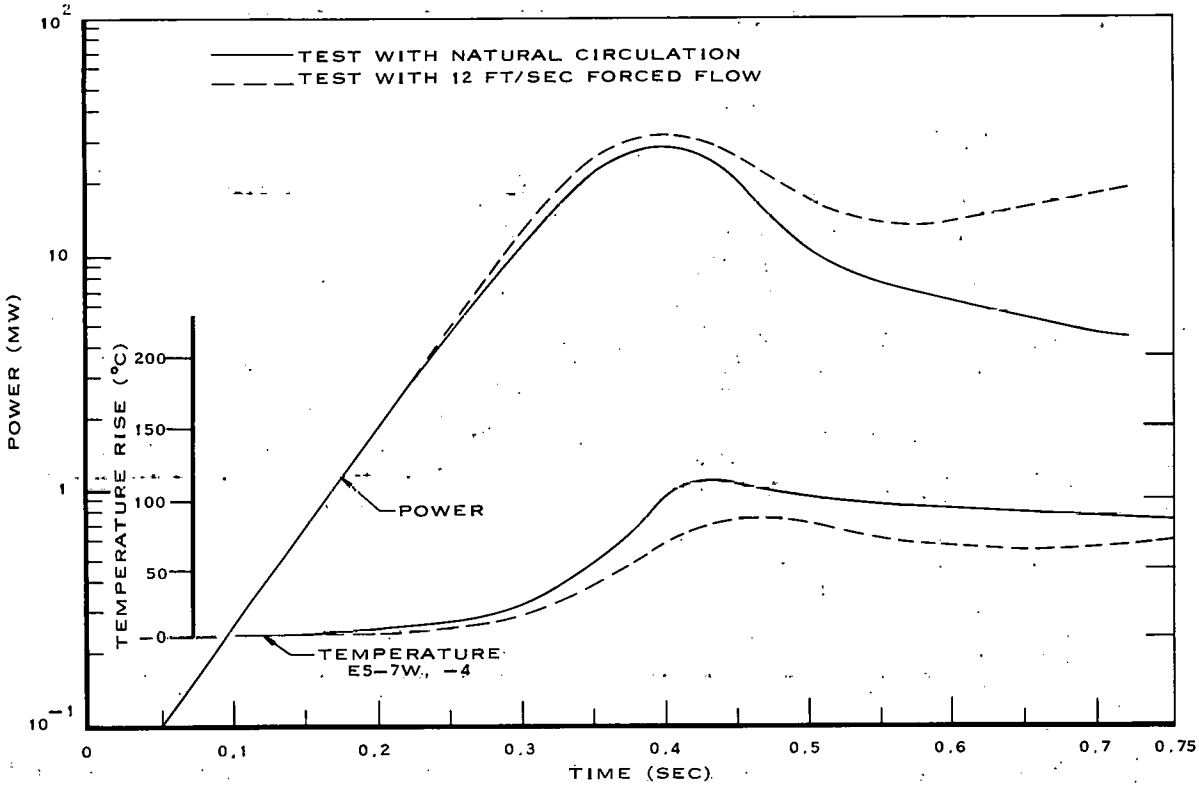

Fig. 29 Reactor power and fuel plate surface temperature for 50-msec-period tests with and without forced coolant flow.

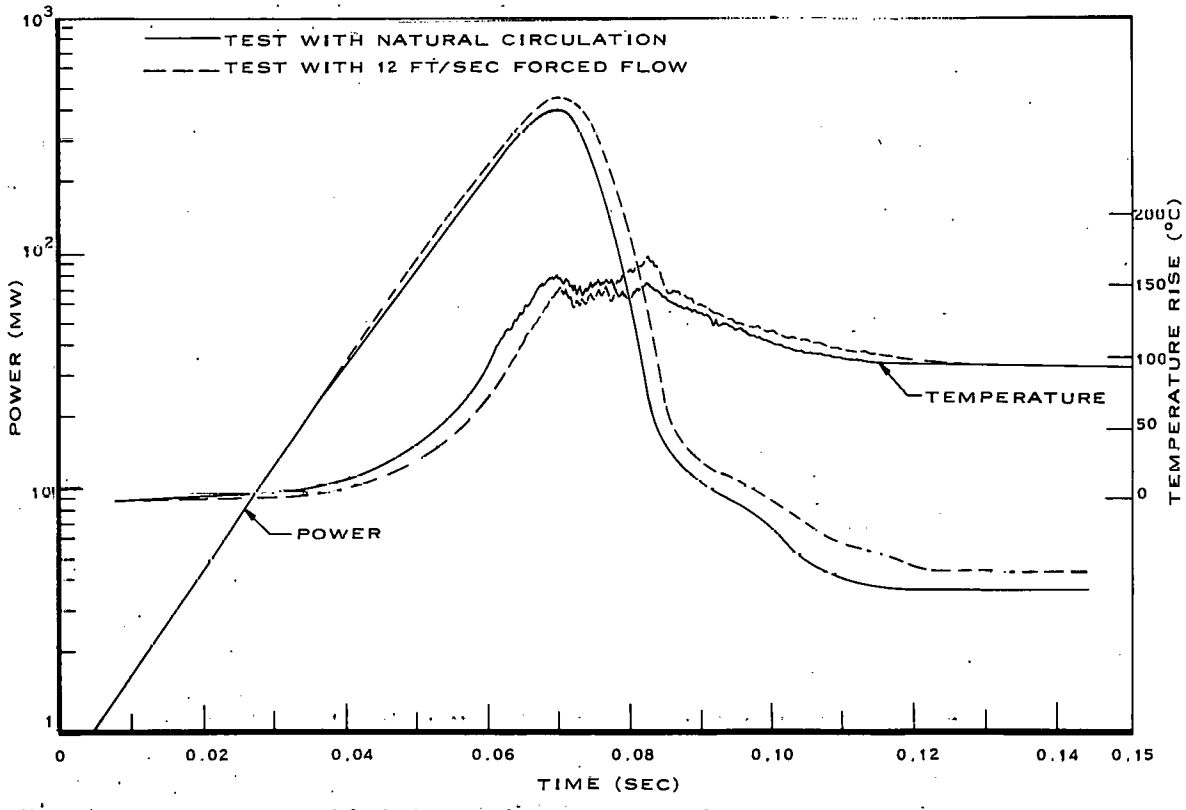

Fig. 30 Reactor power and fuel plate surface temperature for 10-msec-period tests with and without forced coolant flow.

There was no significant difference in transient pressures observed between the tests conducted with and without flow.

5. REDUCED PROMPT NEUTRON LIFETIME (ℓ/β_{eff})

The value of ℓ/β_{eff} for the Spert IV D-12/25 core was determined by analysis of data from a set of 12 step-transient tests. These excursions were performed with no flow and with a flow of 5000 gpm, and with the initial reactivity insertion, R, varied from about 1.1 to 1.8 dollars. The reactivity was inserted essentially as a step by rapid ejection of the transient rod, and the amount of reactivity inserted was determined from a prior reactivity calibration of the control rods. The rod calibration itself was accomplished by long-period measurements, such that the reactivity could be determined by the delayed reactivity term of the inhour relation:

$$R_d(\alpha_o) \approx \sum_i \frac{a_i \alpha_o}{\lambda i + \alpha_o}$$

For shorter-period excursions, the prompt neutron term is significant, and

$$R = \frac{\alpha_o \ell}{k\beta_{eff}} + R_d \qquad (1)$$

where

R = total (prompt and delayed) reactivity ($)

ℓ = prompt neutron lifetime (sec)

$a_i = \beta i_{eff}/\beta_{eff}$

α_o = initial asymptotic reactor period (sec^{-1})

λ_i = i^{th} delayed-neutron-group decay constant

k = static effective multiplication constant

Setting $k = (1 - R\beta_{eff})^{-1} \approx 1 + R\beta_{eff}$, (where, without introducing appreciable error, the value of β_{eff} in the small correction term $R\beta_{eff}$ may be estimated from the buckling) one may rewrite Equation (1) as

$$(R - R_d)(1 + R\beta_{eff}) = \frac{\ell}{\beta_{eff}} \alpha_o$$

Thus, ℓ/β_{eff} is obtained as the slope of the linear plot of $(R - R_d)(1 + R\beta_{eff})$ as a function of α_o. The experimental plot obtained for the Spert IV D-12/25 core is shown in Figure 31. From a least squares linear fit of the data,

$$(\ell/\beta_{eff})\ \text{transient} = (8.1 \pm 0.09) \times 10^{-3}\ \text{sec}$$

where the error represents the standard deviation from the mean.

This value is in good agreement with the value of $(8.1 \pm 0.17) \times 10^{-3}$ sec which had previously been determined [14] by an analysis of the statistical fluctuation of the neutron population in the core for various subcritical multiplication factors.

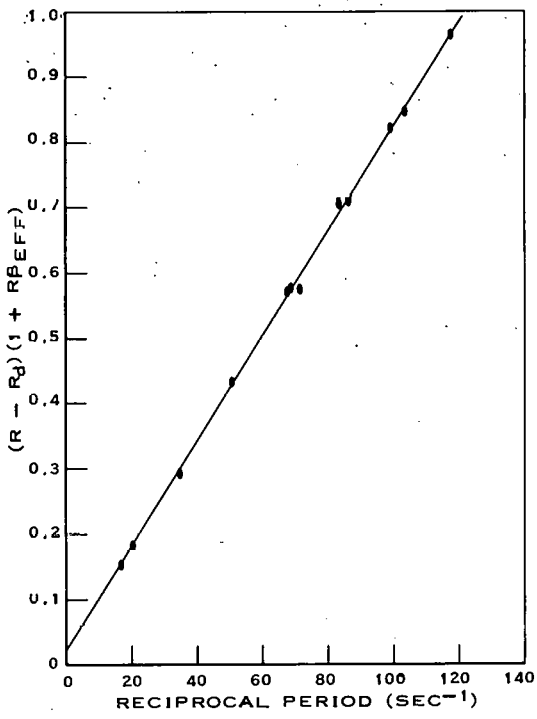

Fig. 31 Prompt reactivity vs reciprocal period for the Spert IV core.

6. TABLE OF TEST RESULTS

Table II presents some of the data from the series of self-limiting excursion tests conducted during the first quarter of 1963.

TABLE II

STEP TRANSIENT TEST DATA FOR SPERT IV D-12/25 CORE

Date (1963)	Run No.	τ (msec)	α_o (sec^{-1})	$\phi(t_m)$ (Mw)	$E(t_m)$ (Mwsec)	$\theta(t_m)$ (°C)	θ(max) (°C)	Head (ft)	Flow (gpm)
February									
12	2	980	1.02	0.77	2.18	70.6	93.0	18	None
14	3	598	1.67	1.12	1.56	67.7	103.0	18	None
19	4	190	5.26	3.32	1.08	63.1	121.0	18	None
21	5	374	2.67	1.55	1.27	68.4	113.0	18	None
25	6	107	9.35	6.9	1.18	73.2	122.0	18	None
26	7	49.8	20.1	25.1	1.83	112.9	124.0	18	None
28	8	29.6	33.8	68.5	3.00	135.9	141.0	18	None
March									
1	9	62.4	16.0	17.5	1.64	99.0	128.0	18	None
5	10	19.6	51.0	147	3.23	147.9	162.0	18	None
6	11	14.5	69.0	247	4.40	165.2	178.0	18	None
7	12	11.7	85.5	350	4.82	175.5	179.0	18	None
8	13	10.15	98.5	467	4.94	182.7	191.0	18	None
11	14	8.48	118.0	615	5.66	170.2	212.0	18	None
12	15	21.3	47.0	145	3.49	131.2	138.0	2	None
13	16	12.0	83.4	340	4.43	155.8	155.0	2	None
14	17	8.83	113.3	570	5.18	164.9	184.0	2	None
15	18	516	1.94	20	—	43.0	93.3	18	5000 (up)
18	19	104	9.62	9.8	1.79	58.4	101.8	18	5000 (up)
19	20	49.3	20.3	30.2	2.71	90.4	107.6	18	5000 (up)
20	21	20.7	48.3	169	4.78	148.8	152.5	18	5000 (up)
21	22	12.2	82.0	370	5.26	167.3	173.1	18	5000 (up)
22	23	10.13	98.7	505	6.08	184.7	192.1	18	5000 (up)

τ ≡ Reactor period

α_o ≡ $1/\tau$

$\phi(t_m)$ ≡ Peak power

$E(t_m)$ ≡ Energy release at time of peak power

$\theta(t_m)$ ≡ Fuel plate surface temperature at time of peak power

θ(max) ≡ Maximum fuel plate surface temperature

III. OXIDE CORE DESIGN STUDY

1. INTRODUCTION

Future program plans for the Spert III and Spert IV facilities include kinetic testing of low-enrichment oxide-rod-type cores typical of those in use or planned for use in the nuclear power industry. A preliminary calculational study has been made preparatory to selection of the fuel design to be used for these future experimental programs.

2. SPERT III OXIDE CORE CALCULATIONS

Tests are planned of a low-enrichment oxide core in the Spert III facility to permit the acquisition of kinetic data for such a core under the primary-coolant system conditions typical of a high-power reactor. For this purpose it is desired to select a fuel-rod and core design which can be accommodated with only minor modifications to the existing facility, and which will provide 2 to 4% available excess reactivity while operating at power at moderator temperatures up to 550°F.

Four-group, one-dimensional diffusion theory calculations have been made for two fuel rod designs: a 4.8 wt% U-235, 0.466-in.-OD fuel rod of the PL-2 type [15] and a 4.5 wt% U-235, 0.34-in.-OD fuel rod of the BR-3 type [16, 17]. Additional data on these fuel rod designs are given in Table III. For each fuel type, calculations were made for four, "metal-to-water" (non-moderator-to-moderator) ratios to determine the core radius required to obtain a k_{eff} of 1.04 at a moderator temperature of 550°F and a core-averaged UO_2 temperature of 2000°F. For the PL-2 type fuel rods, calculations were also made to determine the clean cold excess reactivity of the cores with metal-to-water ratios of 1.0 and 1.25.

The results of these calculations are given in Table IV, and the required core diameters are plotted as a function of the metal-to-water ratio in Figures 32 and 33.

These preliminary results indicate that a suitable core design can be obtained utilizing the PL-2 type fuel rods, and with only slight modifications to the existing Spert III core support structure and control rod drive mechanisms. Two-dimensional neutron diffusion calculations are currently in progress to determine control rod worths, hot excess reactivity, and transient rod worth for a proposed core design using these fuel rods.

3. SPERT IV OXIDE CORE CALCULATIONS

For the future oxide-core test program in the Spert IV facility it is desired to perform kinetic tests with a large diameter core. Preparatory to selection of a fuel rod design for this program, four-group, one-dimensional diffusion theory calculations were performed to determine the k_{eff} of a 7-ft-high by 7-ft-diameter

TABLE III

DATA FOR BELGIAN THERMAL REACTOR (BR-3)
AND PORTABLE LOW-POWER REACTOR (PL-2) FUEL RODS

BR-3 Type Fuel Rods	
Pellet density (g/cm^3)	10.4 (estimate)
Pitch, square (in.)	0.480
Pellet enrichment (wt% U-235)	4.5
Pellet diameter (in.)	0.295
Rod diameter (in.)	0.342
Cladding thickness, type 348 SS (in.)	0.020
Air gap width (in.)	0.004
Rod length (in.)	55.1
PL-2 Fuel Rods	
Pellet density (g/cm^3)	10.50 ± 0.01
Pitch, square (in.)	0.732
Pellet enrichment (wt% U-235)	4.8
Pellet diameter (in.)	0.420
Rod diameter (in.)	0.466
Cladding thickness, type 348 SS (in.)	0.020
Air gap width (in.)	0.003
Rod length (in.)	41.41
Active fuel length (in.)	38.3

cylindrical core with a coolant temperature of 200°F (the maximum operating temperature available for Spert IV) for two fuel rod diameters (0.34 in. and 0.466 in.), for three fuel enrichments (1.5%, 3%, and 4.5%), and for four metal-to-water ratios (0.5, 0.75, 1.0, and 1.25). The results are tabulated in Table V, and shown graphically in Figures 34, 35, and 36. For a metal-water ratio of unity, an enrichment of about 1.65 wt% U-235 is needed to obtain an excess reactivity of 2% for the 0.466-in.-OD fuel rods, and about 2.0 wt% enrichment is required to obtain the same excess reactivity using the smaller rods.

TABLE IV

RESULTS OF SPERT III OXIDE CORE PRELIMINARY DESIGN CALCULATIONS

Fuel Rod Type	Metal/Water Ratio	Core Diameter (in.)	Excess Reactivity (%)
		Hot System	
	Moderator temperature = 550°F, UO_2 temperature = 2000°F		
PL-2	0.50	16.85	4.0
PL-2	0.75	19.13	4.0
PL-2	1.00	22.52	4.0
PL-2	1.25	26.85	4.0
BR-3	0.50	20.16	4.0
BR-3	0.75	24.46	4.0
BR-3	1.00	30.55	4.0
BR-3	1.25	41.57	4.0
		Cold System	
PL-2	1.00	22.52	14.7
PL-2	1.25	26.85	14.1

Temperature Coefficient $C = -2 \times 10^{-4} \frac{\delta k}{k}/°F$

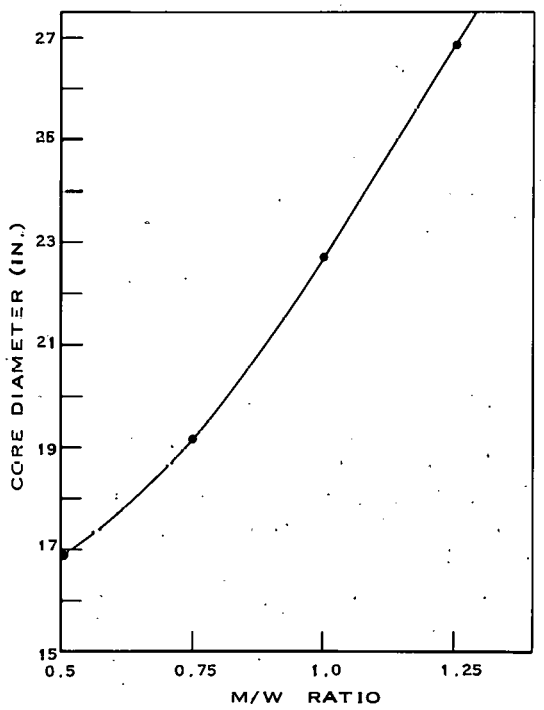

Fig. 32 Core diameter vs metal-to-water ratio, for 4% excess reactivity at moderator temperature of 550°F and UO_2 temperature of 2000°F, for 4.8% enriched, 0.466-in.-OD oxide rods.

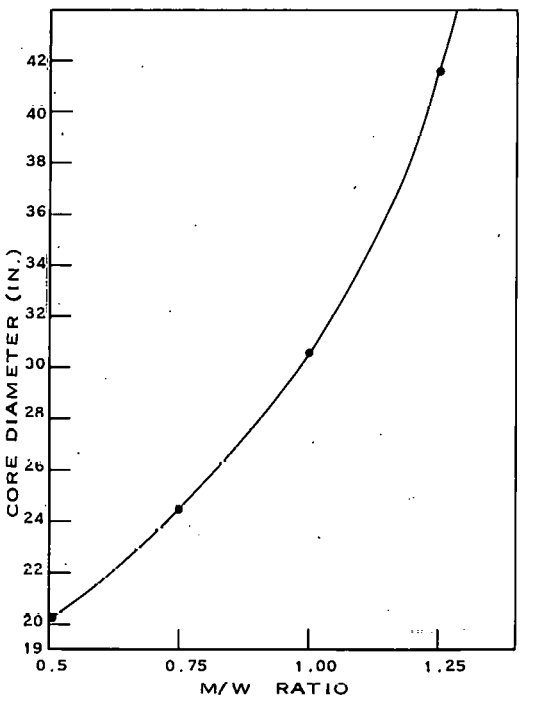

Fig. 33 Core diameter vs metal-to-water ratio for 4% excess reactivity at moderator temperature of 550°F and UO_2 temperature of 2000°F, for 4.5% enriched, 0.34-in.-OD oxide rods.

TABLE V

RESULTS OF SPERT IV OXIDE CORE PRELIMINARY DESIGN CALCULATIONS

Conditions: System temperature = 200°F; 7-ft-high x 7-ft-diameter cylindrical core

Metal/Water Ratio	Enrichment (wt%)	Eigenvalues (k_{eff}) 0.34-in. Pin	0.466-in. Pin
0.5	1-1/2	0.9462	1.0100
0.75	1-1/2	0.9437	1.0187
1.00	1-1/2	0.9277	1.0035
1.25	1-1/2	0.9056	0.9829
0.5	3	1.2106	1.2700
0.75	3	1.1880	1.2531
1.00	3	1.1527	1.2202
1.25	3	1.1210	1.1863
0.5	4-1/2	1.3383	1.3739
0.75	4-1/2	1.3029	1.3558
1.00	4-1/2	1.2602	1.3142
1.25	4-1/2	1.2196	1.2754

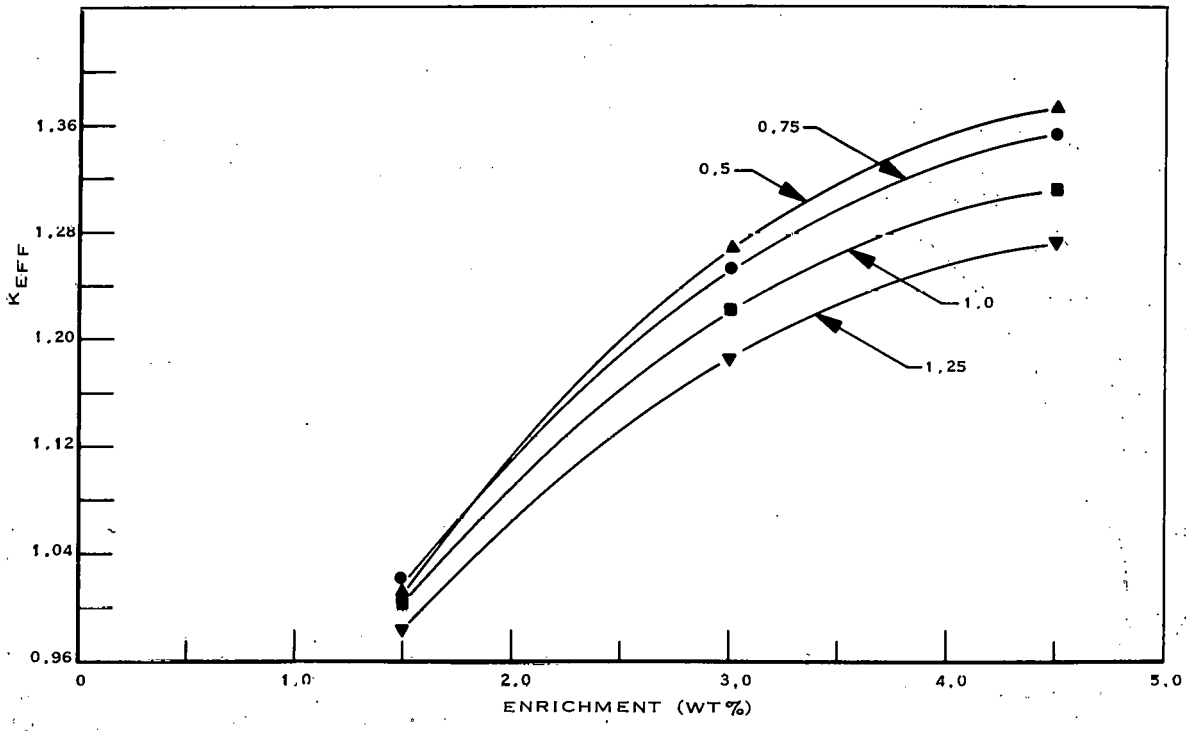

Fig. 34 Plot of k_{eff} vs enrichment for a 7-ft-diameter by 7-ft-high cylindrical core comprised of 0.47-in.-diameter oxide fuel rods, with metal-water ratio as parameter.

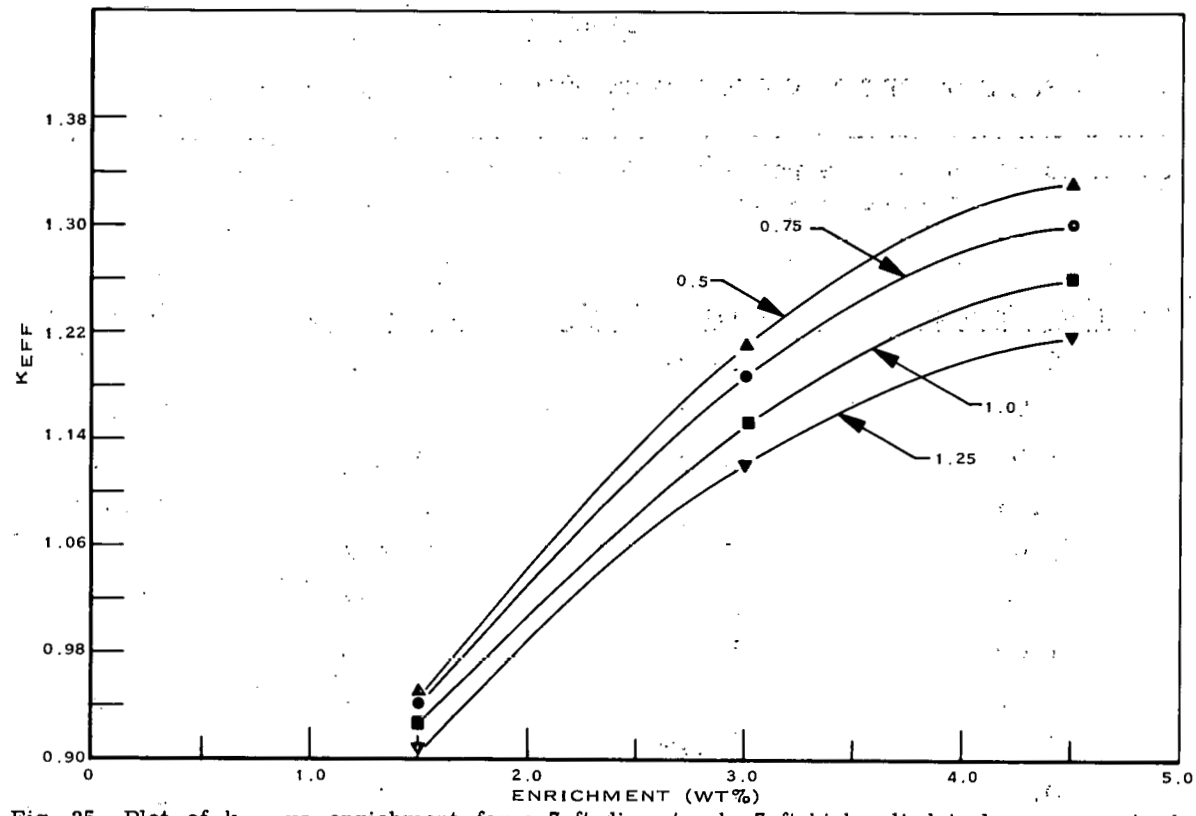

Fig. 35 Plot of k_{eff} vs enrichment for a 7-ft-diameter by 7-ft-high cylindrical core comprised of 0.34-in.-diameter oxide fuel rods, with metal-to-water ratio as parameter.

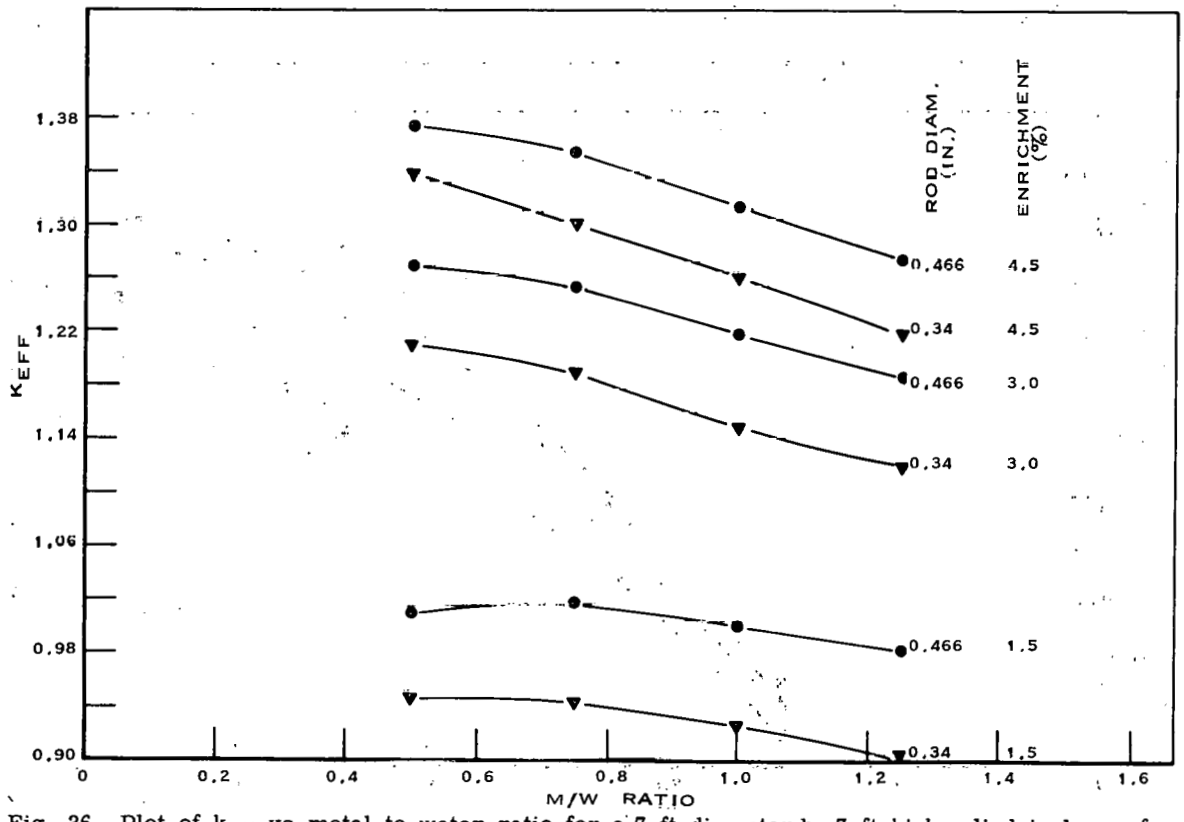

Fig. 36 Plot of k_{eff} vs metal-to-water ratio for a 7-ft-diameter by 7-ft-high cylindrical core for several rod diameters and enrichments.

IV. ANALYSIS

1. ANALYSIS OF DATA FROM HIGH-POWER OSCILLATOR TESTS IN THE SPERT I P-18/19 CORE

In 1959, a series of high-power pile-oscillator experiments was conducted in Spert I with the P-18/19 core in order to measure the frequency response of the reactor to sinusoidal variations in reactivity [18]. The main objective of these tests was to determine the feedback transfer function of the system in order to permit prediction of the limiting power level for reactor stability and to provide a basis for evaluating physical models for the reactivity-compensating mechanisms in the system. Data from high-power oscillator tests performed at a mean power level of 400 kw and a bulk-water temperature of 66°C have now been processed to extract the phase and amplitude of the overall frequency response of the system.

In the performance of these tests, the sinusoidal variation in reactivity was imposed by means of a rotating oscillator rod located in the reflector region adjacent to the core. The amplitude of the reactivity oscillations was about 0.065 dollar, with second and third harmonic content of less than 3% of the fundamental amplitude. The frequency range covered was from 0.002 to 20 cps. The response of the reactor power to the applied reactivity variations was measured by means of a neutron-sensitive ion chamber located adjacent to the core (opposite the oscillator) and was recorded on a photographic oscillograph of the optical galvanometer type. Limited heat-removal capacity (up to about 600 kw) was provided by the installation of auxiliary cooling coils in the reactor tank and by running water directly into and out of the tank and stirring. There was no forced coolant flow through the core. More complete descriptions of the experimental equipment and procedures are given in references 18 and 19.

The principal traces recorded on the oscillograph charts included (a) a phase-reference signal derived from a rotary potentiometer geared to the oscillator drive shaft, (b) the amplified neutron signal from the ion chamber, (c) the neutron signal with the steady-state component balanced out and the time-varying component amplified, and (d) the same as (c), but with high-frequency noise eliminated by means of a low-pass filter.

The balanced neutron-signal traces were digitized by means of a semi-automatic chart reader and a Fourier analysis was performed using an IBM 650 Harmonic Analysis Program (PPCo. 00.009) in order to yield the relative amplitude and phase of the fundamental component of the neutron signal. Various tests were applied to the digitization and Fourier-analysis procedures to ensure that no significant systematic error was introduced by the methods employed. In most cases, ten oscillation cycles were analyzed for each test to improve the accuracy and to obtain an estimate of the uncertainty in the results.

Corrections were applied to the phase data to account for a small frequency-dependent phase lag resulting from mechanical torsion in the oscillator rod, and for the effects of the finite bandwidth of the ion chamber circuit. Corrections were applied to the amplitude data to account for differences in the overall gain of the electronic circuitry and slight differences in the mean power level from run to run. The resulting relative phase and amplitude data were then normalized

to the calculated zero-power transfer function in the frequency range above about 1 cps, where the shapes of the calculated and experimental curves were quite similar.

Figures 37 and 38 show a comparison of the experimental amplitude and phase results at 400 kw and 66°C with the calculated zero-power transfer function. The results are also tabulated in Table VI. The error limits indicated for each data point are estimates of the standard deviation of the mean from the true value. The reproducibility of the measurement at a single frequency (1.5 cps) is seen to be within ± 5%.

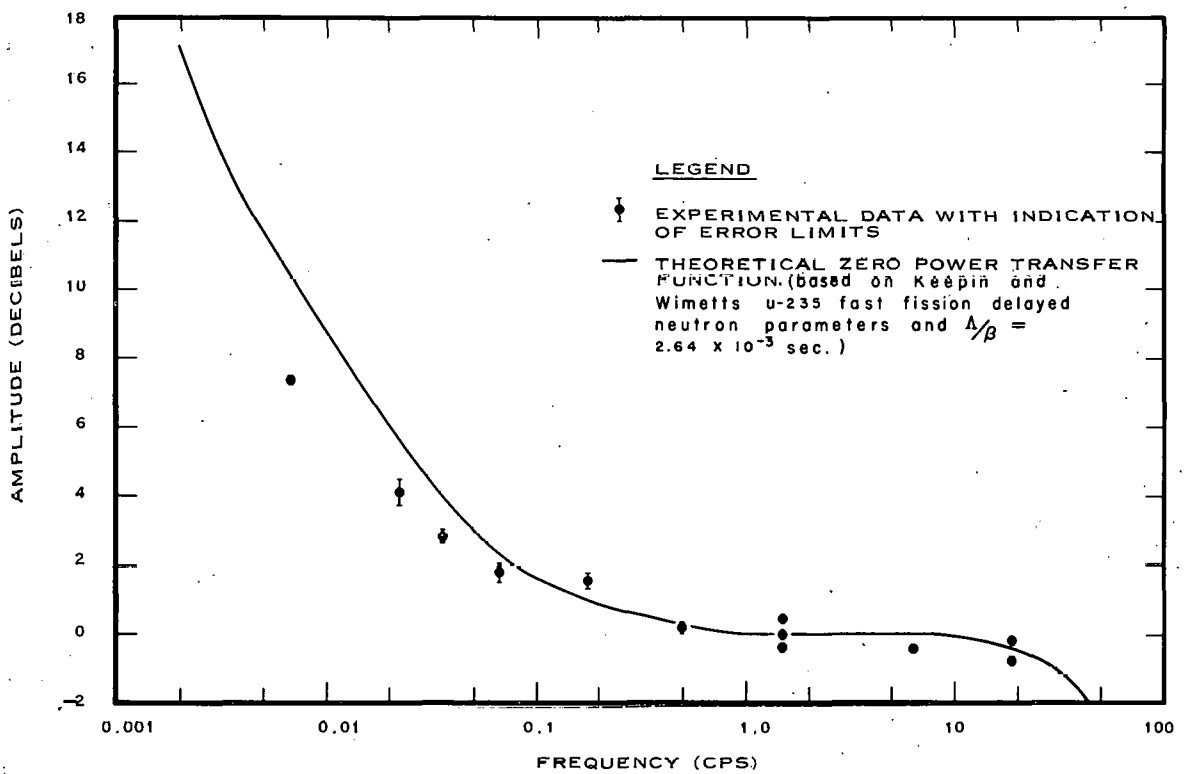

Fig. 37 Amplitude of frequency response of the Spert I P-18/19 reactor at a mean power of 400 kw and a bulk-water temperature of 66°C.

Figures 37 and 38 indicate that the departure of the measured high-power transfer function from the theoretical low-power transfer function is significant only for frequencies below about 1 cps.

Analysis is continuing to extract the feedback transfer function from these data. Once this has been accomplished, an attempt will be made to fit to the resulting curve with analytical expressions which describe the physical processes postulated to be responsible for reactivity feedback in the reactor. In addition, the transfer function results will be used to predict the threshold of reactor instability which will be compared with the results of direct stability tests performed in this reactor. Computational procedures which have been developed to calculate the feedback transfer function directly from the measured step-transient

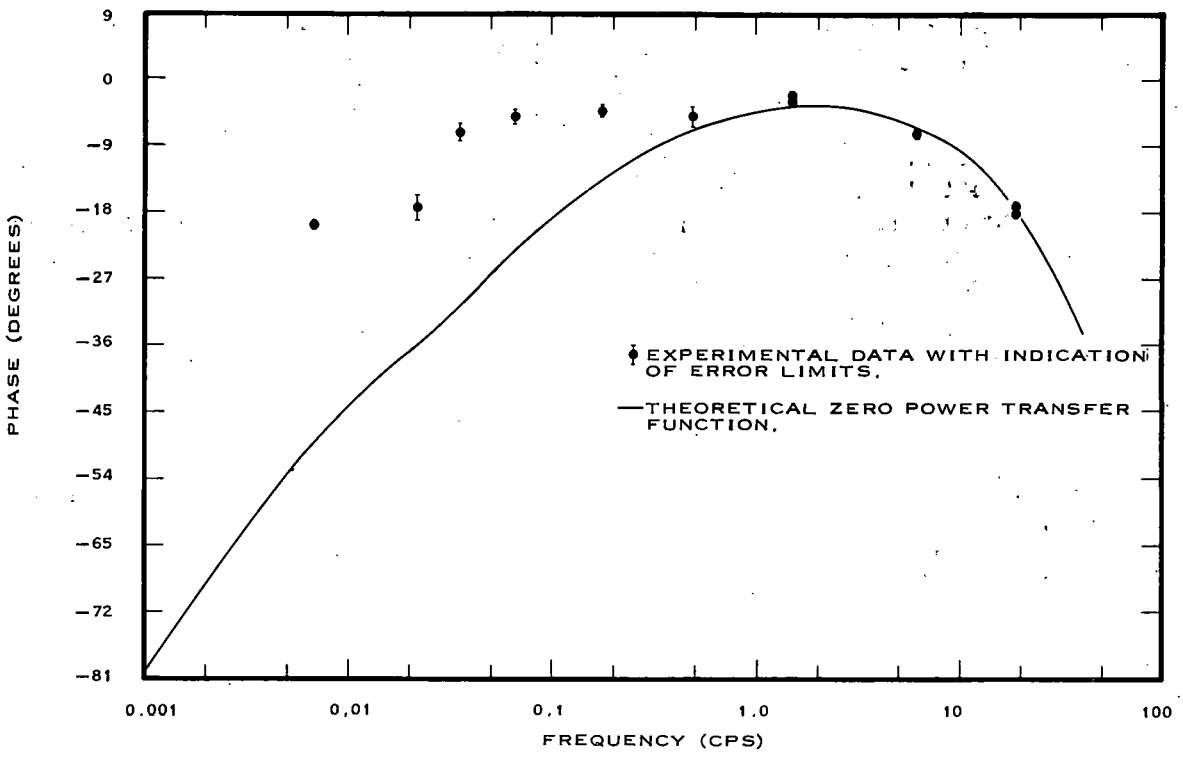

Fig. 38 Phase of frequency response of the Spert I P-18/19 reactor at a mean power of 400 kw and a bulk-water temperature of 66°C.

power response of the reactor (see KERNEL program) will also be tested by comparison with these data.

2. KERNEL PROGRAM

The total reactivity of a reactor is given by the sum

$$r(t) = r_{ex}(t) + r_{fb}(t) \tag{1}$$

where r_{ex} is the externally impressed reactivity and r_{fb} is the feedback component. If linear feedback is assumed, then $r_{fb}(t)$ can be written as

$$r_{fb}(t) = \int_0^t \phi(t-\tau)\, K(\tau) d\tau \tag{2}$$

where $\phi(t)$ is the reactor power. The KERNEL program has been written to calculate K(t) by using the inputs of reactivity and power obtained from the

TABLE VI

COMPARISON OF HIGH-POWER TRANSFER FUNCTION DATA WITH THEORETICAL LOW-POWER TRANSFER FUNCTION

Conditions: Spert I P-18/19 reactor, 400 kw mean power, 66°C bulk-water temperature.

	High-Power Experimental Data		Theoretical Low-Power Data	
Frequency (cps)	Amplitude (db)	Phase (degrees)	Amplitude (db)	Phase (degrees)
0.006836	7.354 ± 0.100	- 19.7 ± 0.433	10.1840	- 48.9
0.02152	3.646 ± 0.355	- 19.5 ± 1.46	5.7606	- 36.4
0.0356	2.792 ± 0.219	- 7.3 ± 1.34	4.0552	- 31.0
0.0662	1.770 ± 0.313	- 5.1 ± 0.85	2.4114	- 23.3
0.177	1.588 ± 0.160	- 4.3 ± 0.95	1.1154	- 13.2
0.491	0.243 ± 0.093	- 5.5 ± 1.36	0.3072	- 7.1
1.48	- 0.352 ± 0.115	- 2.8 ± 0.59	0.0434	- 4.0
1.49	0.523 ± 0.051	- 2.8 ± 0.24	0.0434	- 4.0
1.50	0.000 ± 0.064	- 3.1 ± 0.45	0.0434	- 4.0
6.16	- 0.348 ± 0.028	- 7.2 ± 0.32	- 0.0514	- 6.5
18.4	- 0.273 ± 0.069	- 17.2 ± 0.65	- 0.3954	- 17.2
18.4	- 0.725 ± 0.091	- 17.6 ± 0.58	- 0.3954	- 17.2

REACTIVITY program (see page 43) and the SMOOTH [20] program. K(t) is evaluated at the points $t_{k+1/2} = 0.5\ (t_{k+1} + t_k)$ by the equation

$$K(t_{i+\frac{1}{2}}) = \frac{r_{fb}(t_{i+1}) - \sum_{k=0}^{i-1} K(t_{k+\frac{1}{2}}) \left[g(t_{i+1} - t_k) - g(t_{i+1} - t_{k+1}) \right]}{g(t_1)} \qquad (3)$$

obtained from Equation (2) by application of the extended mean value theorem for integrals. In Equation (3),

$$g(t_i) = \int_0^{t_i} \phi(\tau) d\tau$$

The function K(t), sometimes called the system function, is the impulse response of the feedback system, ie, it is the feedback reactivity which would result from an impulse in the reactor power. Hence, K(t) characterizes the (linear) reactivity feedback system in the time domain in the same manner that the feedback transfer function characterizes the feedback system in the frequency domain. The Laplace transform of K(t) is, of course, the transfer function for reactivity feedback.

The use of K(t), rather than its Laplace transform, to characterize the system has the advantage that K(t) may be computed over a finite time interval from a knowledge of the behavior of the feedback reactivity and the power within the same time interval. To obtain the usual form of the transfer function from the transient response, however, requires that the behavior of the power and the feedback reactivity be known or assumed for all time after initiation of a transient.

3. REVISION OF THE REACTIVITY PROGRAM

As previously reported [21], a computer program was written to calculate reactivity, $\rho(t)$, from the reactor power, $\phi(t)$, using the system of equations

$$\dot{\phi}(t) = \frac{\rho(t) - \bar{\beta}}{\Lambda} \phi(t) + \sum_i \lambda_i C_i(t) \tag{4}$$

$$\dot{C}_i(t) = \frac{\bar{\beta}_i}{\Lambda} \phi(t) - \lambda_i C_i(t) \tag{5}$$

This set of equations is solved for $\$(t) = \rho(t)/\bar{\beta}$, yielding

$$\$(t) = 1 + \frac{\Lambda}{\bar{\beta}} \frac{\dot{\phi}(t)}{\phi(t)} - \sum_i \frac{\lambda_i a_i}{\phi(t)} e^{-\lambda_i t} \int e^{\lambda_i t} \phi(t) dt + \frac{\phi(o)\lambda_i a_i e^{-\lambda_i t}}{\phi(t)(\lambda_i + \alpha)} \tag{6}$$

where $a_i = \bar{\beta}_i/\bar{\beta}$. Thus the calculation of $\$(t)$ from digitized power data involves the numerical evaluation of $\dot{\phi}(t)/\phi(t)$ and $\int e^{\lambda_i t}\phi(t)dt$. As was indicated in reference 21, the numerical solution of Equation (6) was obtained by assuming that, in a small neighborhood of a time point t_j,

$$\phi(t_j + t) = A_j t^2 + B_j t + C_j \tag{7}$$

where A_j, B_j, and C_j are coefficients computed by the SMOOTH program [20].

It has since been determined that the accuracy obtained by this method is insufficient in some cases. Consequently, the program REACTIVITY has been revised to accept coefficients A_j, B_j, and C_j for which

$$\log_e \phi(t_j + t) = A_j t^2 + B_j t + C_j \qquad (8)$$

That is, the coefficients A_j, B_j, and C_j, which are the input to REACTIVITY, correspond to the natural logarithm of the power rather than to the power itself. This system was adopted because of the significance of the quantity $\dot{\phi}/\phi = d/dt(\log_e \phi)$ in Equation (6). The use of the logarithm of the power data permits a more accurate evaluation of this quantity than can be made from linear power data. With this approach, the percent error obtained for a test problem in which the power increased exponentially was decreased by a factor of ≈ 100 from that obtained by the previous approach.

A second test of the revised program was performed by using data from a special transient test performed in Spert I. In this test a reactivity step was first applied, producing an asymptotic period of ≈ 0.3 sec. Then, before the power reached a level high enough to excite the inherent feedback mechanisms in the system, the control rods were inserted at a slow, steady rate to simulate the effect of reactivity feedback. From the previous calibration of the control rods and the known rod position as a function of time, the rate of decrease of reactivity was determined to be $\approx 17¢$/sec. The time history of the reactivity computed by the SMOOTH-REACTIVITY programs agreed with that determined from the rod calibration and the rod position history to within the accuracy of the experiment.

V. REFERENCES

1. Quarterly Technical Report Spert Project, 4th Qtr 1962, IDO-16890 pp 1-18 (1963).

2. Quarterly Technical Report Spert Project, 2nd Qtr 1962, IDO-16806, pp 14-25 (1962).

3. Quarterly Technical Report Spert Project, 3rd Qtr 1962, IDO-16829, pp 5-10 (1963).

4. J. Dugone, D. D. Wieland, Fuel Plate Experience During the Spert I Destructive Test Series with an Aluminum-Clad, Plate-Type Core, IDO-16885 (To be published).

5. G. Long, "Explosions of Molten Aluminum in Water - Cause and Prevention", Metal Progress, 71 pp 107-112 (May 1957).

6. H. M. Higgins, R. D. Shultz, The Reaction of Metals with Water and Oxidizing Gases at High Temperatures, IDO-28000 (April 1957).

7. R. C. Liimatainen et al, Studies of Metal-Water Reactions at High Temperatures. II. Treat Experiments: Status Report on Results with Aluminum, Stainless Steel-304, Uranium, and Zircaloy-2, ANL-6250 (January 1962).

8. Reactor Development Program Progress Report, November 1962, ANL-6658, p 68 (December 1962).

9. A. H. Spano et al, Self-Limiting Power Excursion Tests of a Water-Moderated Low-Enrichment UO_2 Core in Spert I, IDO-16751 (February 1962).

10. A. H. Spano, "Self-Limiting Power Excursion Tests of a Water-Moderated Low-Enrichment UO_2 Core", Nuclear Sci. & Eng., 15, No. 1, pp 37-51 (January 1963).

11. G. O. Bright, S. G. Forbes, Miscellaneous Tests with the Spert I Reactor, IDO-16551 (October 1959).

12. Quarterly Technical Report Spert Project, 4th Qtr 1960, IDO-16687, pp 9-14 (1961).

13. Ibid, pp 14-17.

14. Quarterly Technical Report Spert Project, 4th Qtr 1962, IDO-16890, p 29 (1963).

15. PL Final Design Report. Volume IV. Reactor Design. CEND-135 (Vol. IV), IDO-19030 (June 1961).

16. Directory of Nuclear Power Reactors, Vol. 1, AEC-STI/Publ. No. 4 (June 1959).

17. "Power Reactors and Experiments the World Around", Nucleonics, 19, No. 11, p 132 (1961).

18. A. A. Wasserman, Contributions to Two Problems in Space-Independent, Nuclear-Reactor Dynamics: I. Calculation and Measurement of the Reactor Describing Function. II. Analysis of the Effect of a Reflector or Reactor Dynamics (thesis), IDO-16755 (March 1962).

19. A. A. Wasserman, "High and Low Power Transfer Function Measurements", Proceedings of the Conference on Transfer Function Measurements and Reactor Stability Analysis Held at Argonne National Laboratory, Argonne, Illinois, May 2-3, 1960, ANL-6205 (1960).

20. Quarterly Technical Report Spert Project, 2nd Qtr 1962, IDO-16806, pp 29-30 (1962).

21. Quarterly Technical Report Spert Project, 3rd Qtr 1962, IDO-16829, pp 27-28 (1962).

PHILLIPS
PETROLEUM
COMPANY

ATOMIC ENERGY DIVISION